# Numerical investigation of heat transfer in one-dimensional longitudinal fins

Innocent Rusagara

Reg:367545

Supervised by Prof. Charis Harley

*A thesis submitted to the Faculty of Science in fulfilment of the requirements for degree of Doctor of Philosophy.*

School of Computational and Applied Mathematics.

University of the Witwatersrand, Johannesburg

## Declaration

*I declare that the content of this thesis is original except where due references have been made. It has not been submitted before for any degree to any other institution.*

---

*Innocent Rusagara*

## Dedication

*I dedicate this thesis to my wife and my children.*

## Acknowledgements

*I would like to thank my supervisor Prof. Charis Harley, for all her guidance and for her NRF used fund. I would also like to thank the School of Computational and Applied Mathematics for the two years consecutive offers of the Postgraduate Merit Award.*

## Abstract

In this thesis we will establish effective numerical schemes appropriate for the solution of a non-linear partial differential equation modelling heat transfer in one dimensional longitudinal fins. We will consider the problem as it stands without any physical simplification. The main methodology is based on balancing the non-linear source term as well as the application of numerical relaxation techniques. In either approach we will incorporate the no-flux condition for singular fins. By doing so, we obtain appropriate numerical schemes which improve results found in literature. To generalize, we will provide a relaxed numerical scheme that is applicable for both integer and fractional order non-linear heat transfer equations for one dimensional longitudinal fins.

# Contents

# List of Figures

# List of Tables

## Nomenclature

$A_p$ profile area, $m^2$.

$B$ thermal conductivity parameter.

$c$ specific heat capacity, $J/KgK$.

$c_v$ volumetric heat capacity $2c/(\delta_b A_p)$.

$F(X)$ fin profile, $m^2$.

$f(x)$ dimensionless fin profile.

$H$ heat transfer coefficient, $W/m^2K$.

$h$ dimensionless heat transfer coefficient.

$h_b$ heat transfer at the base, $W/m^2K$.

$K$ thermal conductivity, $W/mK$.

$k$ dimensionless thermal conductivity.

$k_a$ thermal conductivity of the fin at the ambient temperature, $W/mK$.

$L$ length of the fin, $m$.

$n$ exponent.

$P$ fin perimeter, $m$.

$Q$ heat flux, $W/m^2$.

$T$ temperature distribution, $K$.

$T_b$ fin base temperature, $K$.

$T_a$ surrounding temperature, $K$.

$t$ time, $S$.

$X$ Spatial variable, $m$.

$x$ dimensionless spatial variable.

## Greek Symbols

$\beta$ thermal conductivity gradient.

$\delta$ fin thickness, $m$.

$\delta_b$ fin thickness at the base, $m$.

$\eta$ fin efficiency.

$\theta$ dimensionless temperature.

$\mathcal{M}$ thermo-geometric fin parameter.

$\tau$ dimensionless time.

# Chapter 1

# Introduction

The main purpose of this thesis is to provide an effective numerical schemes appropriate for the solution of partial differential equations modelling the non-linear heat transfer in one-dimensional longitudinal fins. This problem is modeled by

$$u_t(x,t) = \nabla_x \left[ f(u(x,t)) \nabla_x u(x,t) \right] - g(u(x,t))$$

where $f(u(x,t))$, and $g(u(x,t))$ are non-linear functions of $u(x,t)$. The equation under consideration has been shown to be difficult to solve especially for special types of profiles such as those defined to be singular [1]. However, their solution is of importance given the wide range of applications for extended surfaces, mostly called fins, in problems considering temperature propagation or heat flow. Obvious examples may be found in several applications of mechanical engineering and in many home appliances [2]. In support of their use, Sparrow and Vemuri [3] have shown that with finned surfaces the heat transfer increases six times in comparison to un-finned surfaces. Kiwan and Al-Nimr [4] proposed the use of porous fins for heat transfer enhancement. Similarly, Kim et al. [5], due to experimental data, advocated the use of porous fins with low permeability and low porosity as plate-porous heat exchang-

ers. Lee et al. [6, 7], when employing sectional oblique fins, illustrated the effective reduction of boundary layer thickness resulting in better heat transfer. Hassanzadeh and Pekel [8] have used functionally graded materials (FGM) for annular fins. Compared to homogeneous fins, the outcome was that FGM annular fins enhanced the heat transfer rates between the annular fin and the surrounding fluids. Jang et al. [9] performed research for the optimum span angle and location of vortex generators in a plate-fin and tube heat exchanger. Furthermore Tao et al. [10] conducted a numerical study of the local heat transfer coefficient and fin efficiency of wavy fin-and-tube heat exchangers.

As can be seen, much research has been conducted regarding the enhancement by considering a variety of different influential factors. Another factor which has import when solving such problems pertains to the 'singularity' of the fin. In such instances it is essential to remember that triangular fin profiles are classified by Kraus [11] as singular. This is due to the fact that it is analytically impossible to characterize them by any linear transformation. Kraus [11] proposed that one assume triangular profiles to be trapezoidal in nature so as to render the problem solvable, however in this manner the original problem becomes oversimplified so as to guarantee a solution to the model. We find that such a methodology may lead to inaccurate results given that fins with trapezoidal profiles are already considered profiles in their own right and as such classified as different profiles entirely. A key feature of the work conducted in this thesis is that we do not simplify the geometry of the fins considered but rather provide a numerical approach that effectively deals with the proper form of the fin.

While much work has been done showing the applicability and thus importance of fins

for heat transfer, solutions are often found for simplified models. It has been found by many researchers that the fin orientation, height, length and spacing in arrays play major roles in the manner and efficiency of heat transfer [12, 13, 14, 15, 16, 17]. Given that these parameters play a fundamental role in the structure of the problem, and even though these inter-linked factors increase the complexity of the problem, they should not be removed for the sake of simplicity. The consequence of this however is that we end up considering a non-linear partial differential equation (PDE), the solution of which cannot always be obtained analytically. In fact, the use of analytical methods has often led to the consideration of a simplified model, especially for complex geometries, whereas this is not necessary when using appropriate numerical methods.

This thesis is outlined as follows. Chapter 1 serves as an Introduction to the work to be discussed and Chapter 2 provides an overview of the physics and construction of the model relevant to the work conducted in this thesis. The model is derived by using Fourier's Law and the first law of thermodynamics. Fundamental steps employed to structure the model are provided as is the non-dimensionalization of the model at hand. After non-dimensionalization we obtain a non-linear heat transfer equation with a non-linear source term; we provide a brief justification for the use of numerical schemes in this case given that their need is well known. However, when using numerical schemes as the solution method it is fundamental to recognize that without a proper numerical treatment of the source term we may not be able to eliminate possible spurious steady state numerical solutions [18]. In fact, if a numerical scheme does not preserve the fundamental balance at the discrete level, this may result in spurious oscillations or 'numerical storms' [19]. In the work of modelling

Lake Rursee at rest [19], it was showed how waves form as pure numerical artifacts. Some of the results were unrealistic and were found to occur due to the use of a non well-balanced numerical scheme and a naive treatment of the source term. In turn, the well-balanced scheme reproduced results for when the lake is at rest extremely accurately. In [20], when modelling gas for sub-orbital Earth re-entry, similar outcomes have been obtained. The test was performed for reacting flows by introducing a small perturbation to the velocity from steady state. The obtained results showed that the non well-balanced schemes responded badly in a very oscillatory fashion while the well-balanced schemes were able to capture the small perturbation excellently. On the other hands, we should deal with simple numerical schemes that can handle discontinuities near steady states. We need schemes that are use neither Riemann solvers spatially nor systems of algebraic equations temporally and that can achieve higher orders of accuracy and pick up weak solutions. Chapter 2 elaborates on these issues and hence paves the way for Chapters 3 and 4 which are dedicated to the implementation of the numerical well-balanced and relaxation schemes respectively.

In Chapter 3 we will focus on an appropriate treatment of the source term of the problem under consideration. The well-balancing approach will be considered and implemented as per the work in [21]. More precisely, this approach is applied to triangular fins which have been characterized by singularities in the literature [1, 11]. It shall be noticed that the no-flux condition along with the well-balancing property are of prime importance in Chapter 3.

For discretization, we implement the finite volume method and illustrate how it reduces the order of differentiation by one. In this manner, by using volume averaging

and the Taylor series expansion, we are able to obtain a numerical balance law. As described in [18, 22, 23], we take advantage of this to establish a balance law from information obtained through a consideration of the steady state equation, which in turn is incorporated into the transient heat transfer equation. This approach is referred to as the well-balancing technique and maintains steady state solutions. It is through this approach that we will obtain solutions to the unsteady heat transfer problem for a triangular fin. Contrary to the suggestion made by Kraus [11], that the profile of the triangular fin should be altered in order to solve the problem under consideration, we maintain the original profile and when implementing the well-balancing approach we incorporate the no-flux condition. In this manner we eliminate any additional assumptions which would usually be required in order to solve the PDE. Rather, we establish a numerical well-balanced scheme via the incorporation of the no-flux condition and we validate the results obtained through the use of benchmark results [1, 24, 25]. This method of solution is novel and to the authors' best knowledge has not been previously used in the literature to solve the problem pertaining to singular fins [26]. Furthermore, the approach used can easily be applied to other singular profiles such as the concave parabolic and convex parabolic profiles.

In Chapter 4 relaxation schemes are investigated as in [27]. In fact, relaxation schemes are commonly seen as simple to deal with and more general in handling discontinuities near steady states. Relaxation uses neither Riemann solvers spatially nor systems of algebraic equation temporally and can achieve higher-order accuracy and pick up the right weak solutions [27]. More generally, relaxation numerical schemes are used in several numerical problems. To cite a few, the research in [28] established a zero relaxation numerical scheme for non-linear hyperbolic conservation laws by constructing

a relaxation system that converts a non-linear conservation law into a system of linear equations with non-linear source terms. The proposed scheme was efficient even when other TVD (Total Variation Diminishing) schemes failed. For the investigated Sod shock tube problem, their relaxation scheme was able to capture the right shock, rarefaction and solve the contact discontinuity. The scheme was able to suppress oscillations and errors were less than the second order accurate Lax-Wendroff scheme [28]. Another example comes from the work in [29] that constructed a relaxation scheme applied to a degenerate diffusion problem. The relaxation approximation helped to reduce the order of the equation and to numerically solve the semi-linear problem. Results provided for second order matched with analytical results and this inspired us to extend the idea to our non-linear heat transfer equation. The only challenge is that our problem seems to be much more complex due to the non-linear nature of the equation coupled with the non-linear source term. This work constitutes a remarkable contribution as no such scheme has been established previously for this problem. The established scheme is applied to heat transfer equations where the fin has an exponential shape profile and results are validated via steady state benchmark solutions [30]. Due to the efficiency and ability of the scheme to achieve higher order accuracy in capturing weak solutions without using Riemann Solvers, the same scheme is also used in Chapter 6. We analyse the convergence of the schemes implemented in Chapters 3 and 4 and compare their results in Chapter 5.

In Chapter 6 we will focus on numerically computing the mean action time. A common question is how long a process takes to reach equilibrium. Several researchers [31, 32, 33] have suggested that one compute an average quantity namely the mean action time in order to answer this question. In their findings, through the use of

initial and final steady state information, it was possible to compute the mean action time without solving the full problem. For processes such as freezing the final steady state temperature is fixed and this process is well known. However, in the instance of heat transfer in fins we are unable to specify the final steady state temperature before the end of the process. This motivates the work conducted in Chapter 5 where a numerical method is used to estimate such mean action times. Suryanarayana [24] tried to obtain the time to steady state but even for a simple linear case, he was unable to compute such a time exactly. Instead, he computed the time $\tau_s$ for which the temperature reaches within one percent of its steady state value. This instance demonstrates clearly the difficulties involved in obtaining such an equilibrium time even for simple linear cases. Our work follows the methodology used in [31, 32] and even so, we do not implement their technique exactly. McNabb and Wake [31] and McNabb [32] focussed on the heat conduction and finite measures for transition times between steady states. One of those finite times was the mean action time associated with the conductive transition from a constant initial temperature to thermal equilibrium at a constant ambient temperature. However, our problem does not provide a final constant temperature such as in freezing processes; rather the final temperature is unknown. In addition, our heat transfer equation is non-linear with a non-linear source term. It is hence impossible to proceed as in [24, 25] or get transformations that may lead us to a Poisson equation to exploit the Green's function properties as done in [31, 32]. This is the key motivation which led us to requiring novel approaches such as the numerical scheme developed in Chapter 4.

In Chapter 7 we investigate the fractional non-linear heat transfer equation. There are many applications of fractional heat transfer equations. Heat transfer in heteroge-

neous media, beam heating, bioheat, and heat arising in fractal transient conduction can be modelled via fractional heat transfer equations [35, 36, 39, 40]. In heterogeneous media, heat transfer can be modelled either by a sub-diffusion or hyper-diffusion equation which results in a fractional order PDE [35]. For heat transfer in skin tissues, the Pennes bioheat model is preferred and it has been recently modelled via a fractional PDE [39]. As none of these articles considered the case of non-linear heat transfer with non-linear source terms, Chapter 7 is an extension of said work. The Chapter introduces fractional calculus systematically with a solid mathematical background focused essentially on necessary tools that assist in establishing the fractional numerical scheme of our non-linear heat equation. This Chapter is an extension of previous Chapters since it combines integer and fractional partial derivatives. The powerful findings of this Chapter have demonstrated that the results obtained in previous Chapters are justified.

Chapter 8 is a conclusion discussing the key achievements and findings of this study as well as highlighting further possible avenues of research.

In this thesis, the aim was to establish effective and efficient numerical schemes appropriate to the solution of non-linear partial differential equations modelling heat transfer in one dimensional longitudinal fins. The true motivation was to further investigate results which have till now been misunderstood - see [1] for details. Via the implementation of appropriate numerical schemes and the proper implementation of the no-flux boundary condition we have been able to solve the model under consideration effectively and efficiently; more importantly we have been able to provide some insights into the unresolved questions posed in [1]. The numerical well-balanced

scheme and the numerical relaxation scheme have been employed due to certain advantages as has already been briefly discussed above. However, in an attempt to explain more fully why standard finite difference schemes or even in-built schemes (such as `pdepe` in MATLAB) have not been employed we elaborate as follows. Simply these schemes have shown an inability to solve a model such as the one posed in this thesis while taking into account the various issues at hand. These issues include the non-linear nature of the PDE, the singularity of the profile, the possibility of producing numerically artificial results, discontinuities near the steady state and possible oscillations in the solutions obtained. As such we turned to the use of the Finite Volume Method, and then more specifically the well-balanced scheme and relaxation scheme. The FVM is an integral approach and can be performed in the presence of piecewise discontinuities whereas standard finite difference schemes cannot be applied under such circumstances. The integral form of the method allows for the order of differentiation to be reduced by one. Given that the model under consideration has a divergence operator enclosing non-linear factors of the temperature gradient, the integral approach can then in a very elegant fashion remove the divergence operator without any difficulty. Furthermore, FVMs unlike finite difference methods are not limited to discrete point values as they employ higher-order local cell moments. Hence these methods are able to simulate problems with large gradients or jump discontinuities in non-linear conservation laws [60]. As a last point in favour of the use of FVMs it is important to note that previous standard finite difference schemes employed for the solution of models describing the heat transfer in singular fins (see [1] and references therein) were unable to maintain the adiabatic condition. The FVM made the proper implementation of this condition effortless.

More particularly the well-balanced and relaxation schemes have been strongly supported in the literature [18, 19, 20, 21, 22, 23, 27, 28, 29]. The well-balanced scheme has been shown to be powerful when solving partial differential equations (with different structures) while avoiding numerical artifacts. In turn, the relaxation has been strongly advocated given the avoidance of Riemann solvers and its ability to manage discontinuities near steady states. Furthermore, the method has been shown to suppress oscillations - see [28]. In either case, the schemes have been validated by comparisons to analytical results in the literature and their use has been extended to the computation of the time taken to reach the steady state. As such, the work done in this thesis has provided novel approaches for the solution on models such as the one under discussion. As will be discussed later there is still scope for further research in terms of establishing the analytical stability and convergence of the methods.

# Chapter 2

# Derivation of model equation

## 2.1 General introduction

The energy occurring as an outcome of a temperature gradient is referred to as heat transfer and this temperature difference is taken as a major force leading to heat flow. It is natural that heat flows from hot objects to cold ones [41]. Heat transfer occurs in three mechanisms namely: conduction, convection and radiation [11, 41]. Specifically, conduction is defined as the transfer of heat in solids and fluids without bulk motion while the convection is defined as a heat transferred between a solid surface and the adjacent fluid that is in motion. Lastly, radiation is quite different since it does not require a medium of transfer. It is the transfer of energy, passing in different directions at the speed of light.

The purpose of this Chapter is to discuss the derivation of the model which will be the focus of this thesis and in so doing justify the use of numerical schemes for its solution.

### 2.1.1 Fourier's Law of heat conduction

The heat flux $\overrightarrow{q}$, resulting from thermal conduction is proportional to the magnitude of the temperature gradient and opposite to it in sign [41, 42].

This means that

$$\overrightarrow{q} \quad \alpha \quad -\overrightarrow{\nabla} T. \tag{2.1}$$

Let $k$ be the coefficient of proportionality, then

$$\overrightarrow{q} = -k\overrightarrow{\nabla} T. \tag{2.2}$$

In one dimension we have

$$q = -k\frac{\partial T}{\partial x}. \tag{2.3}$$

The coefficient of proportionality $k$ is referred to as the thermal conductivity parameter. It is clearly seen that Fourier's law involves two dependent variables $T$ and $q$. It is best to eliminate $q$ from the equation by using the first law of thermodynamics and the heat transfer rate.

### 2.1.2 First law of thermodynamics

As highlighted by Lienhard IV and Lienhard V [41], the heat transfer rate $Q$ is provided by

$$Q = \frac{dU}{dt} + w_k \tag{2.4}$$

with $\frac{dU}{dt}$ the rate of change of the internal thermal energy, and $w_k$ the work transfer rate, where $\frac{dU}{dt} = mc_v\frac{\partial T}{\partial t}$ with $m = \rho A dx$ the mass, $c_v$ the specific heat capacity, $A$ the surface area, and $\rho$ defined as the density. Therefore,

$$Q = mc_v\frac{\partial T}{\partial t} + w_k$$

Figure 2.1: *Heat flow process*

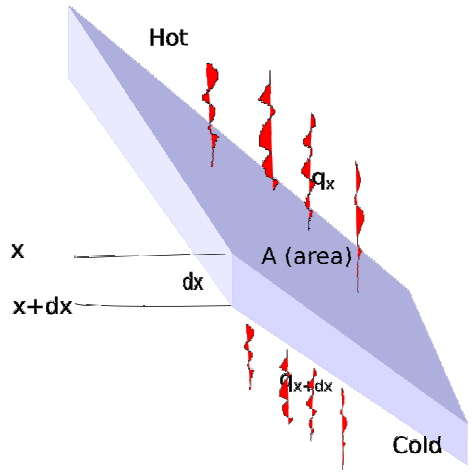


That is

$$Q = \rho A c_v \frac{\partial T}{\partial t} dx + w_k. \tag{2.5}$$

In Fig. 2.1.1, we simulate the heat transfer rate computation from a flux $q(x)$ at $x$ and $q(x + dx)$ at $x + dx$ traversing an area $A$ of width $dx$. The heat traversing the surface area $A$ of width $dx$ is provided by

$$Aq(x + dx) - Aq(x) = \frac{Aq(x + dx) - Aq(x)}{dx} dx.$$

From equation (2.3) we have $q(x) = -k\dfrac{\partial T(x)}{\partial x}$ and $q(x + dx) = -k\dfrac{\partial T(x + dx)}{\partial x}$. Hence, the total heat transfer rate that goes out is provided by

$$Q = \frac{\partial}{\partial x}\left(kA\frac{\partial T}{\partial x}\right) dx. \tag{2.6}$$

From equation (2.5) and (2.6) we have

$$\frac{\partial T}{\partial t} = \frac{1}{\rho A c_v}\frac{\partial}{\partial x}\left(kA\frac{\partial T}{\partial x}\right) + S. \tag{2.7}$$

where $S = -\dfrac{w_k}{\rho A c_v dx}$ is a source term generated by the work done from the thermal energy supplied to the system. This can come from the heat transferred to the sur-

rounding fluid by convection that depends on the heat transfer coefficient given by the power law used in most of industrial applications [43].

Equation (2.7) is referred to as a heat diffusion equation with source term. The purpose of this Section was to sketch the heat transfer processes by use of fundamental laws of thermodynamics to model different types of heat transfer like conduction and convection. It serves as a powerful introduction and it provides the needed mathematical tools used in the remaining part of this thesis. From this structure, we are able to expand the model to consider the heat transfer within longitudinal fins, as per the next Section.

## 2.2 Mathematical model formulation

We consider a longitudinal one-dimensional fin with a profile area $A_p$ referred to wedge-shaped fins by Kraus [11]. The perimeter of the fin is denoted by $P$ and the length of fin by $L$. The fin is attached to a fixed base surface of temperature $T_b$ and extends into a fluid of temperature $T_a$. The fin profile is given by the function $F(X)$, and the fin thickness at the base is $\delta_b$. The energy balance for a longitudinal fin is given by [11]

$$\rho c_v \frac{\partial T}{\partial t} = A_p \frac{\partial}{\partial X}\left(F(X)K(T)\frac{\partial T}{\partial X}\right) - PH(T)\left(T - T_a\right), \quad 0 < X < L \tag{2.8}$$

where $K$ and $H$ are the non-uniform thermal conductivity and heat transfer coefficient depending on the temperature (see e.g. [34, 44, 45, 46]). The fin length is measured from the tip to the base as shown in Fig. 2.2 (see also, [11, 44, 45]). An insulated fin at one end with the base temperature at the other implies boundary conditions are

Figure 2.2: *Schematic representation of a longitudinal fin with arbitrary profile* $F(X)$.

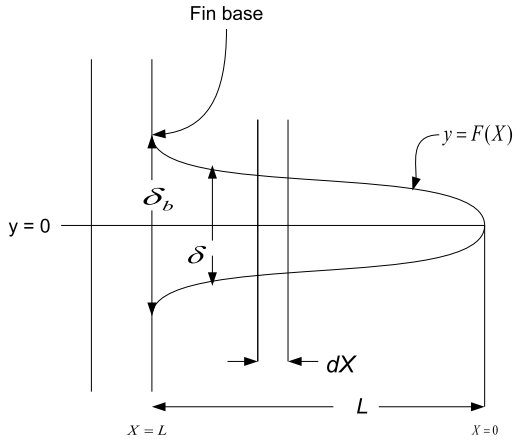


given by [11]

$$T(t, L) = T_b, \qquad \text{and} \qquad \frac{\partial T}{\partial X}\Big|_{X=0} = 0 \tag{2.9}$$

and initially the fin is kept at the temperature of the fluid (the ambient temperature)

$$T(0, X) = T_a. \tag{2.10}$$

Introducing the dimensionless variables

$$x = \frac{X}{L},\ \tau = \frac{k_a t}{\rho c_v L^2},\ \theta = \frac{T - T_a}{T_b - T_a},\ h = \frac{H}{h_b},\ k = \frac{K}{k_a},$$

$$\mathcal{M}^2 = \frac{2Ph_bL^2}{k_a\delta_b A_p} \qquad \text{and} \qquad f(x) = \frac{2}{\delta_b}F(X), \tag{2.11}$$

then equation (2.8) reduces to the relevant dimensionless energy equation given by

$$\frac{\partial\theta}{\partial\tau} = \frac{\partial}{\partial x}\left[f(x)k(\theta)\frac{\partial\theta}{\partial x}\right] - \mathcal{M}^2\theta h(\theta), \quad 0 < x < 1. \tag{2.12}$$

The above equation represents the non-linear heat transfer equation when the thermal conductivity and heat transfer coefficients depend on temperature. The heat transfer coefficient is given by the power law used in most industrial applications [1, 43] as

$$H(T) = h_b\left(\frac{T - T_a}{T_b - T_a}\right)^n. \tag{2.13}$$

The exponent $n$ varies between $-6.6$ and 5, however it tends to lie between $-3$ and 3 in most practical applications [1]. Furthermore, the thermal conductivity of the fin is assumed to vary linearly with the temperature [1] as is the case for many engineering applications. As such we find that

$$K(T) = k_a\left[1 + \beta\left(T - T_a\right)\right] \tag{2.14}$$

which in dimensionless variables gives $k(\theta) = 1 + B\theta$ where $B = \beta\left(T_b - T_a\right)$ is nonzero with $\beta$ as the thermal conductivity gradient. However, we should not exclude the case where the thermal conductivity parameter follows the power law of the temperature profile. In that case, $k(\theta) = \theta^m$ [30].

Hence, the dimensionless heat transfer equation for a longitudinal one-dimensional fin is given by [1, 24, 25]

$$\frac{\partial\theta}{\partial\tau} = \frac{\partial}{\partial x}\left(f(x)k(\theta)\frac{\partial\theta}{\partial x}\right) - \mathcal{M}^2\theta^{n+1}, \qquad 0 < x < 1, \quad \tau \geq 0 \tag{2.15}$$

where boundary conditions are as follows

$$\frac{\partial \theta}{\partial x}\Big|_{x=0} = 0 \qquad \text{at the fin tip} \tag{2.16}$$

and

$$\theta(\tau, 1) = 1, \qquad \text{at the base} \tag{2.17}$$

with initial condition

$$\theta(0, x) = 0. \tag{2.18}$$

It is very important to point out that equation (2.15) is not easy to solve in general; given that our choices for $f(x)$ and $k(\theta)$ heavily affect the equation's solvability. In fact, the ease of the equations solution can vary depending on the choice made for these functions. All types of fin profiles that are mentioned in this thesis are defined in Table 2.1. It is also crucial to recognize the effect of non-linearity as a major contributor to the complexity of the problem. The purpose of this thesis is to appropriately solve this equation as it stands without simplification to maintain all effects of the original problem. As per the work of Noelle et al. [19], a numerical scheme that does not preserve the fundamental balance at discrete level may result in spurious oscillations or numerical storms. In the literature - see for instance [11] - models describing fins with singular profiles (such as triangular fins) were simplified so as to assure their solution; in turn when the model was considered as it stands the use of inappropriate methods and the inappropriate implementation of the adiabatic condition lead to the latter not being maintained in the solutions obtained [1]. In the Chapter that follows we provide a novel means for the solution of the model under consideration which overcomes these problems.

Table 2.1: *Types of fin profiles mentioned in the thesis*

| Types | Fin profile function |
|---|---|
| Rectangular | $f(x) = 1, \quad 0 \leq x \leq 1$ |
| Triangular | $f(x) = x, \quad 0 \leq x \leq 1$ |
| Concave parabolic | $f(x) = x^2, \quad 0 \leq x \leq 1$ |
| Convex parabolic | $f(x) = \sqrt{x}, \quad 0 \leq x \leq 1$ |
| Exponential | $f(x) = e^{\alpha x}, \quad 0 \leq x \leq 1$ |

# Chapter 3

# Numerical well-balanced scheme

*The work conducted in this Chapter has been published in the Journal of Mathematical Problems in Engineering* [26].

## 3.1 Introduction

In this Chapter, we consider a one dimensional non-linear heat transfer equation of the form

$$\theta_t + F_x = Q(\theta) \tag{3.1}$$

with

$$F_x = \frac{\partial}{\partial x}\left(f(x)k(\theta)\frac{\partial \theta}{\partial x}\right)$$

and

$$Q(\theta) = \mathcal{M}^2\theta^{n+1}.$$

For the homogeneous case where $Q(\theta) = 0$, the case is simpler. In fact, many numerical schemes were conceived so as to solve non-reactive flows [47] which is the case when $Q(\theta) = 0$. For similar equations in conservation laws with source terms,

fraction step splitting methods are most used and can be structured for our case as follows

$$\theta_t + F_x = 0 \tag{3.2}$$

and

$$\theta_t = Q(\theta) \tag{3.3}$$

which excludes the inclusion of the source term into the numerical scheme [21]. According to Leveque [47], the fraction step splitting method has successfully been used for many problems. However, when $\theta_t$ is small with respect to $F_x$ and $Q(\theta)$, the solution is close to steady state where $F_x$ and $Q(\theta)$ should balance exactly [21]. Therefore, the accurate solution for a transient equation must rely on this balancing rule principle. It has been highlighted by Leveque that fractional step methods may fail [21]. On the other hand, aside from the fractional step method, Leveque [47] has indicated that most of the numerical algorithms used in solving problems related to reacting flows were conceived to solve problems related to non-reacting flows and hence those schemes perform quite poorly to preserve steady states due to the presence of source terms. Therefore, a well-balanced numerical scheme preserving steady state solutions is more appropriate for solving transient equation with source term. In this Chapter we focus on well-balanced numerical schemes for one dimensional non-linear heat transfer equations with source terms. For further reading, the well-balanced method is well described in [18, 20, 21, 23, 47, 48, 49, 50].

In this Chapter, we have applied a well-balanced numerical scheme to triangular fins which had been characterized as singular profiles in the literature [11, 1]. When solving the problem of heat transfer in a triangular geometry it is essential to remember that triangular fin profiles have been classified by Kraus et al. [11] among

singular profiles because it is analytically impossible to characterize them by any linear transformation. In much research the triangular fin has been considered in an inappropriate manner due to a misunderstanding of the unusual physics of the problem, especially when pertaining to the tip of the fin. Through a consideration of unsuitable boundary conditions the numerical solution of the problem had led to inaccurate and unusual results - see [1] for such discussions. Through an incorporation of the zero-flux boundary condition however, we eliminated any additional assumptions which would usually be required in order to solve the PDE. Rather, we established a numerical well-balanced scheme via the incorporation of the zero-flux condition and we validated the results obtained through the use of benchmark results [1, 24, 26, 30]. This method of solution is novel and to the authors best knowledge has not previously been used in the literature to solve the problem of singular fins. Furthermore, the approach used can easily be applied to other singular profiles such as the concave parabolic and convex parabolic profiles.

## 3.2 Numerical approach

### 3.2.1 The Finite Volume Method and Numerical Balance Law

At first we intend to briefly introduce the manner in which we will employ the finite volume method (FVM) and its advantages within the context of heat transfer problems. In this scenario, due to its integral approach, the FVM reduces the order of the spatial derivative by one. This motivates its use for the heat transfer equation under consideration given the presence of a second derivative in its conduction term.

In current case, we would consider the partial differential equation of the form

$$\frac{\partial\theta}{\partial\tau} - \frac{\partial}{\partial x}\left(g(x,\theta)\frac{\partial\theta}{\partial x}\right) = q(\theta) \tag{3.4}$$

where $g(x,\theta) = f(x)k(\theta)$ is a function of $x$ and the thermal conductivity $k$, involved in the convective term, and $q(\theta) = -\mathcal{M}^2\theta^{n+1}$ a function from the heat transfer coefficient, which represents the source term.To discretise the spatial grid we define the points $x_{i+\frac{1}{2}}$ with mesh width $\Delta x_i = x_{i+\frac{1}{2}} - x_{i-\frac{1}{2}}$ as well as the time step $\Delta\tau_j = \tau_{j+1} - \tau_j$ such that $\theta_i^j$ denotes the approximation cell average of $\theta$ in the cell $\left[x_{i-\frac{1}{2}}, x_{i+\frac{1}{2}}\right]$ at time $\tau_j$ while $\theta^j_{i+\frac{1}{2}}$ is the approximation of $\theta$ at $x = x_{i+\frac{1}{2}}$ and $\tau = \tau_j$.

In order to reduce the order of the spatial derivatives by one we integrate equation (3.4) over the grid cell $[x_{i-\frac{1}{2}}, x_{i+\frac{1}{2}}]$ to obtain

$$\int_{x_{i-\frac{1}{2}}}^{x_{i+\frac{1}{2}}} \frac{\partial\theta}{\partial\tau}dx - \int_{x_{i-\frac{1}{2}}}^{x_{i+\frac{1}{2}}} \frac{\partial}{\partial x}\left(g(x,\theta)\frac{\partial\theta}{\partial x}\right)dx = \int_{x_{i-\frac{1}{2}}}^{x_{i+\frac{1}{2}}} q(\theta)dx.$$

By cell averaging we find that

$$\Delta x_i \frac{d\tilde{\theta}_i(\tau)}{d\tau} - \left(g(x,\theta)\frac{\partial\theta}{\partial x}\right)\Bigg|_{x_{i-\frac{1}{2}}}^{x_{i+\frac{1}{2}}} = \int_{x_{i-\frac{1}{2}}}^{x_{i+\frac{1}{2}}} q(\theta)dx \tag{3.5}$$

where

$$\tilde{f}_i = \frac{1}{\Delta x_i}\int_{x_{i-\frac{1}{2}}}^{x_{i+\frac{1}{2}}} f dx \tag{3.6}$$

is the cell-averaged quantity of $f$ over the grid cell $[x_{i-\frac{1}{2}}, x_{i+\frac{1}{2}}]$. It is obvious that the order of the partial differential equation under consideration has been reduced by one and this increases the accuracy of the results we are to obtain.

In the next Section we will employ the numerical approach described above for equation (2.15) and in so doing develop a numerical balance law of (3.5). In this manner

we obtain a well-balanced scheme which preserves specific non-trivial steady state solutions and may help to minimize some of the oscillations which occur around steady states [20]. Thus for the more general heat transfer equation (3.4) a well-balanced scheme can provide a solution that must satisfy

$$\frac{\partial}{\partial x}\left(g(x,\theta)\frac{\partial\theta}{\partial x}\right) = q(\theta)$$

for steady states. An easily understandable and effective procedure has been established by Wang [18] which will be implemented in this work for the one-dimensional heat transfer problem given by equation (2.15). It should also be kept in mind that this methodology may easily be extended to higher dimensions.

### 3.2.2 Numerical well-balanced scheme

In considering equation (2.15) we find that the one dimensional steady heat equation for regular fins is expressed by

$$\frac{d}{dx}\left(f(x)k(\theta)\frac{d\theta}{dx}\right) = \mathcal{M}^2\theta^{n+1},\ \ 0 < x < 1, \tag{3.7}$$

$$\frac{d\theta}{dx}\Big|_{x=0} = 0,\ \ \theta(1) = 1.$$

Integrating over the grid cell $\left[0,\ \ x+\frac{\Delta x}{2}\right]$, as discussed previously within the context of the FVM, we obtain

$$\int_0^{x+\frac{\Delta x}{2}}\left(\frac{d}{dx}\left(f(x)k(\theta)\frac{d\theta}{dx}\right)\right)dx = \mathcal{M}^2\int_0^{x+\frac{\Delta x}{2}}\theta^{n+1}dx,\ \ 0 < x < 1,$$

which is equivalent to

$$\left(f(x+\frac{\Delta x}{2})k\left(\theta(x+\frac{\Delta x}{2})\right)\right)\frac{d\theta(x+\frac{\Delta x}{2})}{dx} = \mathcal{M}^2\int_0^{x+\frac{\Delta x}{2}}\theta^{n+1}dx,\ \ 0 < x < 1. \tag{3.8}$$

Similarly over $[0, x - \frac{\Delta x}{2}]$ we find that

$$\left(f(x - \frac{\Delta x}{2})k\left(\theta(x - \frac{\Delta x}{2})\right)\right)\frac{d\theta(x - \frac{\Delta x}{2})}{dx} = \mathcal{M}^2 \int_0^{x-\frac{\Delta x}{2}} \theta^{n+1} dx, \;\; 0 < x < 1. \quad (3.9)$$

From mean value theorem we have

$$\int_0^{x+\frac{\Delta x}{2}} \theta^{n+1} dx = \left(x + \frac{\Delta x}{2}\right)\theta^{n+1}(\varphi), \;\; 0 < \varphi < x + \frac{\Delta x}{2}. \quad (3.10)$$

A Taylor series approximation of $\theta^{n+1}(\varphi)$ around $x$ provides

$$\theta^{n+1}(\varphi) = \theta^{n+1}(x) + (n+1)(\varphi - x)\theta^n(x)\frac{d\theta}{dx} + o\left((\varphi - x)^2\right) \quad (3.11)$$

where $o$ stands for the order of accuracy here and in the whole remaining part of this thesis when applicable. Hence,

$$\int_0^{x+\frac{\Delta x}{2}} \theta^{n+1} dx = \left(x + \frac{\Delta x}{2}\right)\left(\theta^{n+1}(x) + (n+1)(\varphi - x)\theta^n(x)\frac{d\theta}{dx} + o\left((\varphi - x)^2\right)\right). \quad (3.12)$$

For $\varphi \to x + \frac{\Delta x}{2}$ we have

$$\int_0^{x+\frac{\Delta x}{2}} \theta^{n+1} dx = \left(x + \frac{\Delta x}{2}\right)\left(\theta^{n+1}(x) + (n+1)\frac{\Delta x}{2}\theta^n(x)\frac{d\theta}{dx} + o\left(\Delta x^2\right)\right). \quad (3.13)$$

Similarly

$$\int_0^{x-\frac{\Delta x}{2}} \theta^{n+1} dx = \left(x + \frac{\Delta x}{2}\right)\left(\theta^{n+1}(x) - (n+1)\frac{\Delta x}{2}\theta^n(x)\frac{d\theta}{dx} + o\left(\Delta x^2\right)\right). \quad (3.14)$$

Therefore

$$\int_{x-\frac{\Delta x}{2}}^{x+\frac{\Delta x}{2}} \theta^{n+1} dx = \Delta x\left(\theta^{n+1}(x) + (n+1)x\theta^n(x)\frac{d\theta}{dx} + o\left(\Delta x^2\right)\right). \quad (3.15)$$

### 3.2.3 Balance law

From (5.2) we have

$$\int_0^x \frac{d}{dx}\left(f(x)k(\theta)\frac{d\theta}{dx}\right)dx = \mathcal{M}^2\int_0^x \theta^{n+1}dx \tag{3.16}$$

which is equivalent to

$$f(x)k(\theta(x))\frac{d\theta(x)}{dx} = \mathcal{M}^2\int_0^x \theta^{n+1}dx. \tag{3.17}$$

By mean value integral theorem and Taylor series approximation we have

$$\begin{aligned} &f(x)k(\theta(x))\frac{d\theta(x)}{dx} = \mathcal{M}^2 x\theta^{n+1}(\varphi),\ \ 0<\varphi<x \\ &= \mathcal{M}^2 x\left(\theta^{n+1}(x) + (n+1)(\varphi - x)\theta^n(x)\frac{d\theta}{dx} + o\left((\varphi-x)^2\right)\right). \end{aligned} \tag{3.18}$$

For $\varphi \to x - \dfrac{\Delta x}{2}$ and $\Delta x$ very small we have

$$f(x)k(\theta(x))\frac{d\theta(x)}{dx} = \mathcal{M}^2 x\left(\theta^{n+1}(x) - (n+1)\frac{\Delta x}{2}\theta^n(x)\frac{d\theta}{dx} + o\left(\Delta x^2\right)\right). \tag{3.19}$$

Hence,

$$\frac{d\theta}{dx} = 2\mathcal{M}^2 x\left(\frac{\theta^{n+1}}{2f(x)k(\theta(x)) + (n+1)\mathcal{M}^2\Delta x x\theta^n(x)} + o\left(\Delta x^2\right)\right). \tag{3.20}$$

From the equations (3.15) and (3.20), the source term balancing law can be established as follows

$$\int_{x-\frac{\Delta x}{2}}^{x+\frac{\Delta x}{2}} \theta^{n+1}dx = \Delta x\left(\theta^{n+1}(x) + \frac{2(n+1)\mathcal{M}^2x^2}{2f(x)k(\theta(x)) + (n+1)\mathcal{M}^2\Delta x x\theta^n(x)}\theta^{2n+1}(x) + o\left(\Delta x^2\right)\right). \tag{3.21}$$

Integrating equation (2.15) over $\left[x-\frac{\Delta x}{2}, x+\frac{\Delta x}{2}\right]$ and incorporating expression (3.21) into the resulting expression we obtain

$$\frac{\partial\theta}{\partial\tau} = \frac{1}{(\Delta x)^2}\left\{f(x+\frac{\Delta x}{2})k(\theta(x+\frac{\Delta x}{2}))\frac{\partial\theta(x+\frac{\Delta x}{2})}{\partial x} - f(x-\frac{\Delta x}{2})k(\theta(x-\frac{\Delta x}{2}))\frac{\partial\theta(x-\frac{\Delta x}{2})}{\partial x}\right\}$$
$$-\mathcal{M}^2\left(\theta^{n+1}(x) + \frac{2(n+1)\mathcal{M}^2x^2}{2f(x)k(\theta(x)) + (n+1)\mathcal{M}^2x\Delta x\theta^n(x)}\theta^{2n+1}(x)\right). \tag{3.22}$$

We now substitute finite difference approximations to our derivatives into equation (3.22). We consider $\left[x_i-\frac{\Delta x}{2}, x_i+\frac{\Delta x}{2}\right]$ for a particular time $t_j$ which provides us with the following approximations

$$\frac{\partial\theta(x_i+\frac{\Delta x}{2})}{\partial x}\Big|_j = \frac{\theta^j(x_i+\Delta x)-\theta^j(x_i)}{\Delta x} = \frac{\theta^j_{i+1}-\theta^j_i}{\Delta x}$$
$$\frac{\partial\theta(x_i-\frac{\Delta x}{2})}{\partial x}\Big|_j = \frac{\theta^j(x_i)-\theta^j(x_i-\Delta x)}{\Delta x)} = \frac{\theta^j_i-\theta^j_{i-1}}{\Delta x}$$
$$\frac{\partial\theta}{\partial\tau}\Big|_i = \frac{\theta^{j+1}_i-\theta^j_i}{\Delta t}.$$

Hence, our well-balanced numerical scheme is given by the following recurrence relation

$$\theta^{j+1}_i = \theta^j_i + \frac{\Delta t}{(\Delta x)^2}\left[f_{i+\frac{1}{2}}k(\theta^j_{i+\frac{1}{2}})(\theta^j_{i+1}-\theta^j_i) - f_{i-\frac{1}{2}}k(\theta^j_{i-\frac{1}{2}})(\theta^j_i-\theta^j_{i-1})\right]$$
$$-\Delta t\mathcal{M}^2\left((\theta^j_i)^{n+1} + \frac{2(n+1)\mathcal{M}^2x_i^2}{2f_ik(\theta^j_i)+(n+1)\mathcal{M}^2x_i\Delta x(\theta^j_i)^n}(\theta^j_i)^{2n+1}\right) \tag{3.23}$$

where a linear interpolation is used to determine $f_{i+\frac{1}{2}}$, $f_{i-\frac{1}{2}}$, $\theta_{i+\frac{1}{2}}$ and $\theta_{i-\frac{1}{2}}$.

**No-flux at origin**

In order to implement our well-balanced numerical scheme we need to first incorporate the relevant boundary conditions. According to the work by Kraus [11], some fins' shapes require special interpretation - a clear example thereof is the triangular fin

profile. Longitudinal fins of triangular profile have been classified among singular fins that cannot be characterized by any linear transformation. As such it is important to remember that the fin profile tapers to zero thickness at the tip and hence there will be a zero flux at this point. This means that

$$\frac{\partial}{\partial x}\left(f(x)k(\theta)\frac{\partial\theta}{\partial x}\right)\Big|_{x=0}=0. \tag{3.24}$$

We now implement a time forward discretisation at the origin and employ the no-flux condition given by (3.24) to obtain

$$\theta_0^{j+1}=\theta_0^j-\Delta t\mathcal{M}^2\left(\theta_0^j\right)^{n+1}. \tag{3.25}$$

As one can see the physical reality of zero thickness at the tip complicates the solution of the problem. If one were to only employ the no-flux condition, given the initial condition of zero temperature, one would always have a zero temperature at the origin as per (3.25). This does not make physical sense however, given that after a considerable time the temperature would be expected to increase at the tip of the fin. At this stage we turn to the well-balancing principle as a means of overcoming this problem.

We employ the well-balancing principle at the origin as a means of incorporating the expression of $\theta_0^j$ into equation (3.25). As such, we consider the steady sate equation as follows

$$\int_{x_0}^{x_0+\frac{\Delta x}{2}}\frac{d}{dx}\left(f(x)k(\theta)\frac{d\theta}{dx}\right)dx=\frac{\Delta x}{2}\mathcal{M}^2\theta^{n+1}(x_0)$$

$$f(x_0+\frac{\Delta x}{2})k(\theta(x_0+\frac{\Delta x}{2}))\frac{d}{dx}\theta(x_0+\frac{\Delta x}{2})-f(x_0)k(\theta(x_0))\frac{d\theta}{dx}(x_0)=\frac{\Delta x}{2}\mathcal{M}^2\theta^{n+1}(x_0)$$

$$f(x_0+\frac{\Delta x}{2})k(\theta(x_0+\frac{\Delta x}{2}))\frac{d}{dx}\theta(x_0+\frac{\Delta x}{2})-0=\frac{\Delta x}{2}\mathcal{M}^2\theta^{n+1}(x_0),\ \text{because}\ \frac{d\theta}{dx}(x_0)=0$$

$$f(x_0+\frac{\Delta x}{2})k(\theta(x_0+\frac{\Delta x}{2}))\frac{d}{dx}\theta(x_0+\frac{\Delta x}{2})=\frac{\Delta x}{2}\mathcal{M}^2\theta^{n+1}(x_0).$$

Through the use of a central difference approximation we then obtain

$$\theta_0^j=\theta_1^j-\frac{\Delta x^2}{2f(x_{\frac{1}{2}})k(\theta_{\frac{1}{2}}^j)}\mathcal{M}^2(\theta_0^j)^{n+1}. \tag{3.26}$$

The coupled equations (3.25) and (3.26) provide a numerical well-balanced discretisation for a triangular fin profile at the origin.

**Flux at origin**

For regular fin profiles the flux at the origin is non-zero and adiabatic conditions are governed by the boundary conditions. At the origin we have

$$\frac{\partial\theta}{\partial\tau}-f(x)k(\theta)\frac{\partial^2\theta}{\partial x^2}+\mathcal{M}^2(\theta)^{n+1}\bigg|_{x=0}=0\ \ \text{because}\ \ \frac{d}{dx}\left(f(x)k(\theta)\right)\frac{d\theta}{dx}(x_0)=0$$

Implementing the forward difference approximation for time and the central difference approximation for space we find that

$$\theta_0^{j+1}=\theta_0^j-\frac{2\Delta\tau f(x_0)k(\theta_0^j)}{\Delta x^2}(\theta_1^j-\theta_0^j)+\Delta\tau\mathcal{M}^2(\theta_0^j)^{n+1} \tag{3.27}$$

and using similar finite difference approximations on the steady state equation of regular fins we obtain

$$\theta_0^j=\theta_1^j-\frac{\Delta x^2}{2f(x_0)k(\theta_0^j)}\mathcal{M}^2(\theta_0^j)^{n+1}. \tag{3.28}$$

Equations (3.27) and (3.28) summarize the discretisation at the origin for regular fin profiles.

## 3.3 Results and discussion

### 3.3.1 Triangular fin profiles

As stated earlier, previous researches have proposed that one approximate the shape of triangular fins by considering the trapezoidal profile as a means of facilitating linear transformations. Aside from proposed simplifications, work has also been done while maintaining the profile in its original triangular form. In [1] for instance, numerical solutions were obtained for the heat transfer in a triangular fin which did not maintain the adiabatic condition - this was thought to be due to thermal instability within the fin as discussed in Yeh and Liaw [43].

The importance of the work conducted here is that the numerical scheme developed did not rely on any simplifying assumptions as proposed by Kraus [11]. Furthermore, the results obtained in [1] are shown to be due to an inaccurate methodology, specifically related to the boundary conditions for profiles which lead to singularities. In applying the no-flux condition in a novel manner we were able to obtain a recursive scheme able to capture the true behaviour of the model under consideration.

We obtained numerical solutions via our well-balanced scheme to equation (2.15) for a triangular fin profile with $B = 1$, $n = 1$, $\mathcal{M} = 0.01, 1, 1.5$, and $\mathcal{M} = 5$ at different values of $\tau$. Figures 3.1 and 3.2 indicate that the temperature decreases from the base to tip of the fin and that the temperature at the tip increases with time. These results make physical sense and also match the behaviour of the temperature distribution found for other fin profiles. Interestingly, for small values of time $\tau$ the response

temperature is virtually independent of the value of $\mathcal{M}$ and this is why a single curve is shown for $\tau = 0.0001$, $\tau = 0.001$, and $\tau = 0.01$. This has been explained in Suryanarayana [24] where it is said that at small values of $\tau$, the bulk of the thermal energy entering at the base remains stored in the fin with only a small fraction available for dissipation through surface convection. Thus, the heat transfer coefficient has very little direct impact on the temperature profile - rather its impact may be related to the length of the fin which in turn influences the temperature profile [1].

In turn, as $\tau$ increases it is seen that the role of convection and hence $\mathcal{M}$ becomes progressively significant as shown by Figure 3.3 and Figure 3.4. Another point is that the steady state is reached quicker for longer fins or fins with higher values of $\mathcal{M}$ as shown by Figure 3.2 for $\tau = 0.5$. This same Figure 3.2 shows clearly that at $\tau = 0.5$ only a stationary state has been reached for the fin profile where $\mathcal{M} = 5$, which is the largest value chosen. This is a consequence of the fact that the dimensionless time $\tau = \dfrac{k_a t}{\rho c L^2}$ should decrease with an increase in $\mathcal{M}$.

While the numerical results we have obtained for the heat transfer in triangular fins matches those obtained by Suryanarayana [24] for other types of fin profiles in linear cases we still require further verification of our results. The results provided in [24] in and of itself cannot justify the accuracy of the results obtained via our well-balanced numerical scheme given the fact that no other concrete analysis currently exists and that all previous attempts at obtaining solutions for the triangular case were done with reservations regarding the results obtained [1]. For this reason, our model has been applied to the rectangular case, where we do have confirmed results, as a means of validating the scheme implemented.

### 3.3.2 Model validation

For a rectangular fin profile the solution profiles from our well-balanced numerical scheme are depicted by the Figures 3.5, 3.6 and 3.7. It is clearly visible that the temperature is an increasing function of time and it decreases from the base to the tip. Figure 3.5 depicts the effect of the thermo-geometric fin parameter on the temperature. We can see that the temperature is a decreasing function of $\mathcal{M}$. In contrast, the temperature distribution is an increasing function of parameter $n$ as shown by Figure 3.7. What is important to realise is that the results we have obtained for the rectangular case via the well-balanced scheme employed for the triangular case, verify the benchmarks results of [1, 24] and hence act as a validation of our well-balanced numerical scheme.

## 3.4 Conclusion

The well-balanced numerical scheme which we have established in this work has been shown to effectively and efficiently obtain results for the rectangular fin profile, matching previous results found in the literature [1, 24, 30]. Our discretisation incorporates the flux condition for the rectangular case as is appropriate, however for the triangular fin profile we incorporated the no-flux condition into our established well-balanced numerical scheme and this constitutes the originality of our work.

Several researchers [30, 46] have proposed some exact solutions, but the main problem was that they were simplifying the problem by adjusting the geometric form of the fin as a means of guaranteeing analytical solutions. Kraus[11] for example, suggested one assume triangular profiles to be trapezoidal so as to guarantee the existence of

linear transformations.

In our work however, such simplifications are not needed. The well-balanced numerical scheme which we developed is able to handle the triangular case without any assumption due to the incorporation of the appropriate conditions, namely the no-flux condition. This approach can easily be extended to other singular profiles, such as the convex and concave parabolic profiles, and hence it constitutes a clear path to a generalized numerical scheme for the solution of problems in heat transfer.

Figure 3.1: *A triangular fin profile with* $B = 1, n = 1,\ \mathcal{M} = 0.01,\ \mathcal{M} = 1,\ \mathcal{M} = 1.5,$ *and* $\mathcal{M} = 5$ *for* $\tau = 0.0001(top)$ *and* $\tau = 0.001(bottom)$.

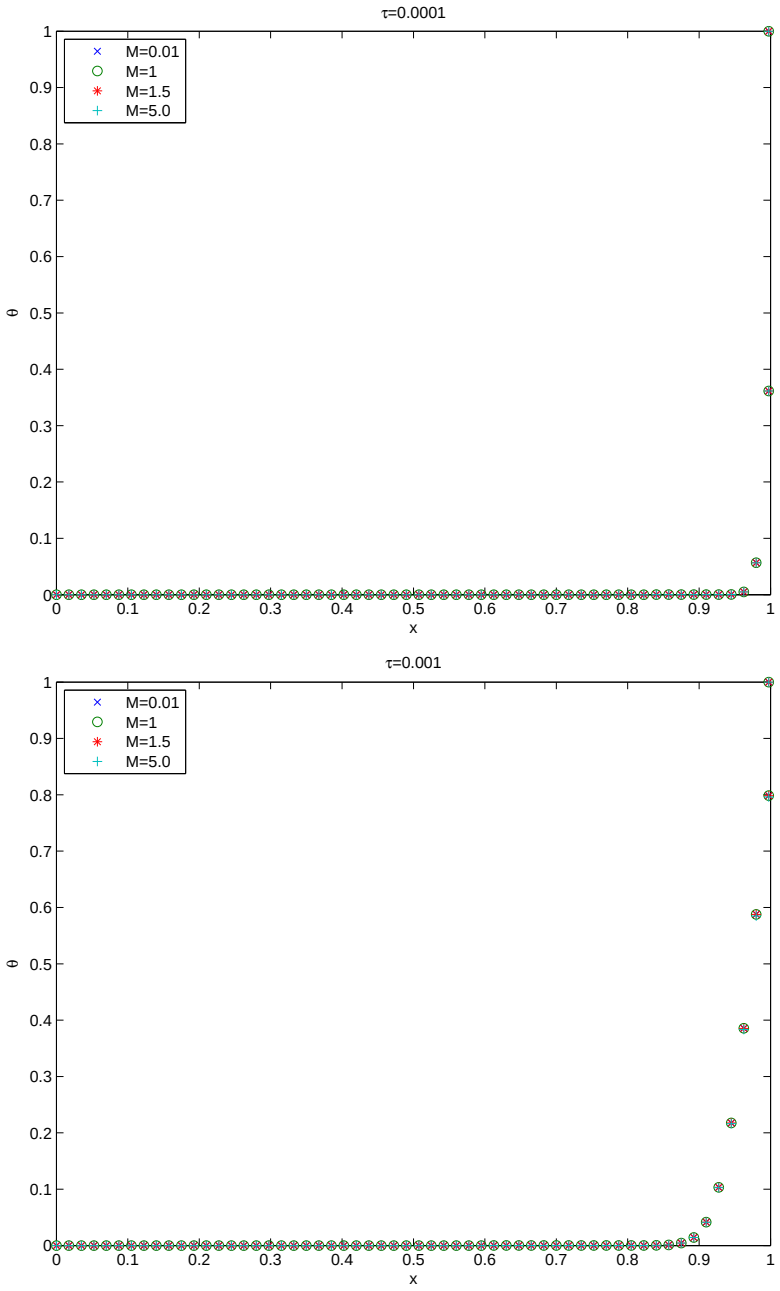

Figure 3.2: *A triangular fin profile with* $B = 1,\ n = 1,\ \mathcal{M} = 0.01,\ \mathcal{M} = 1,\ \mathcal{M} = 1.5,$ *and* $\mathcal{M} = 5$ *for* $\tau = 0.1(top)$ *and* $\tau = 0.5(bottom)$.

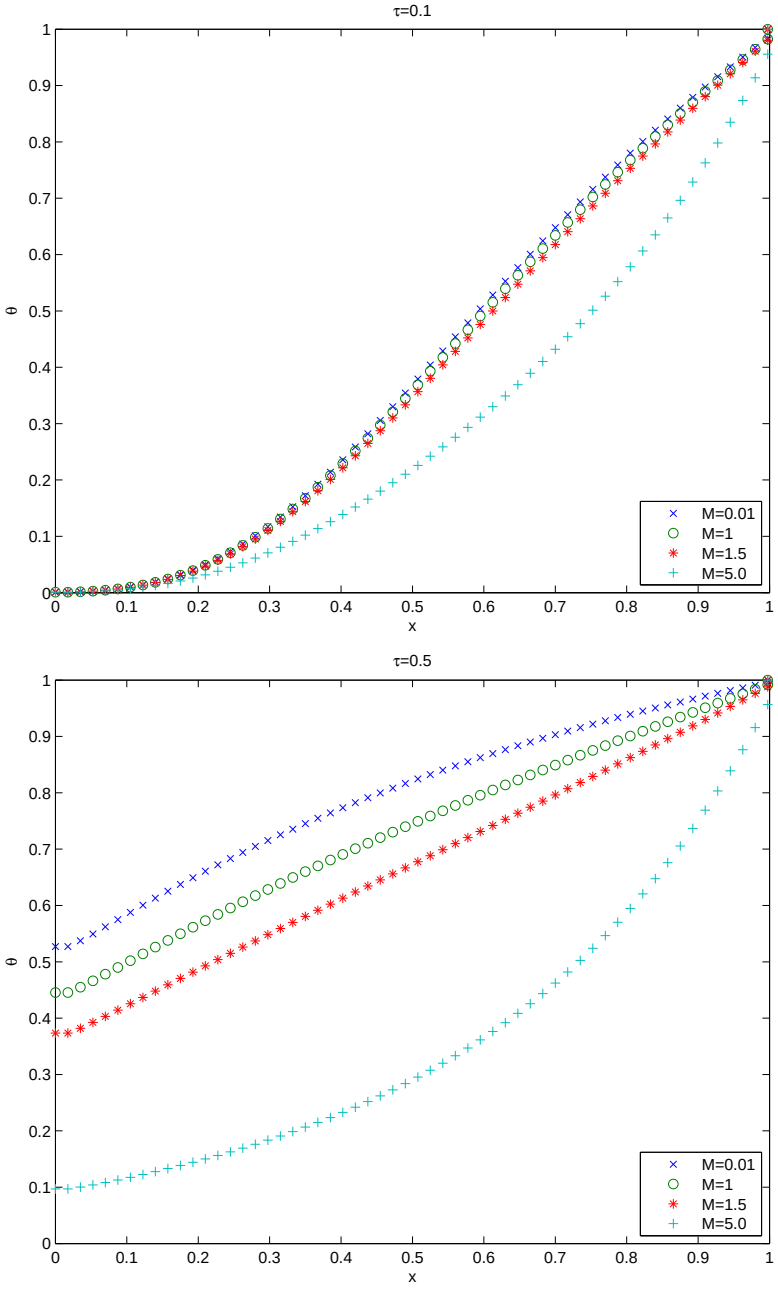

Figure 3.3: *A triangular fin profile with* $B = 1,\ n = 1,\ \mathcal{M} = 0.01,\ \mathcal{M} = 1,\ \mathcal{M} = 1.5,$ *and* $\mathcal{M} = 5$ *for* $\tau = 0.75(top)$ *and* $\tau = 1(bottom)$.

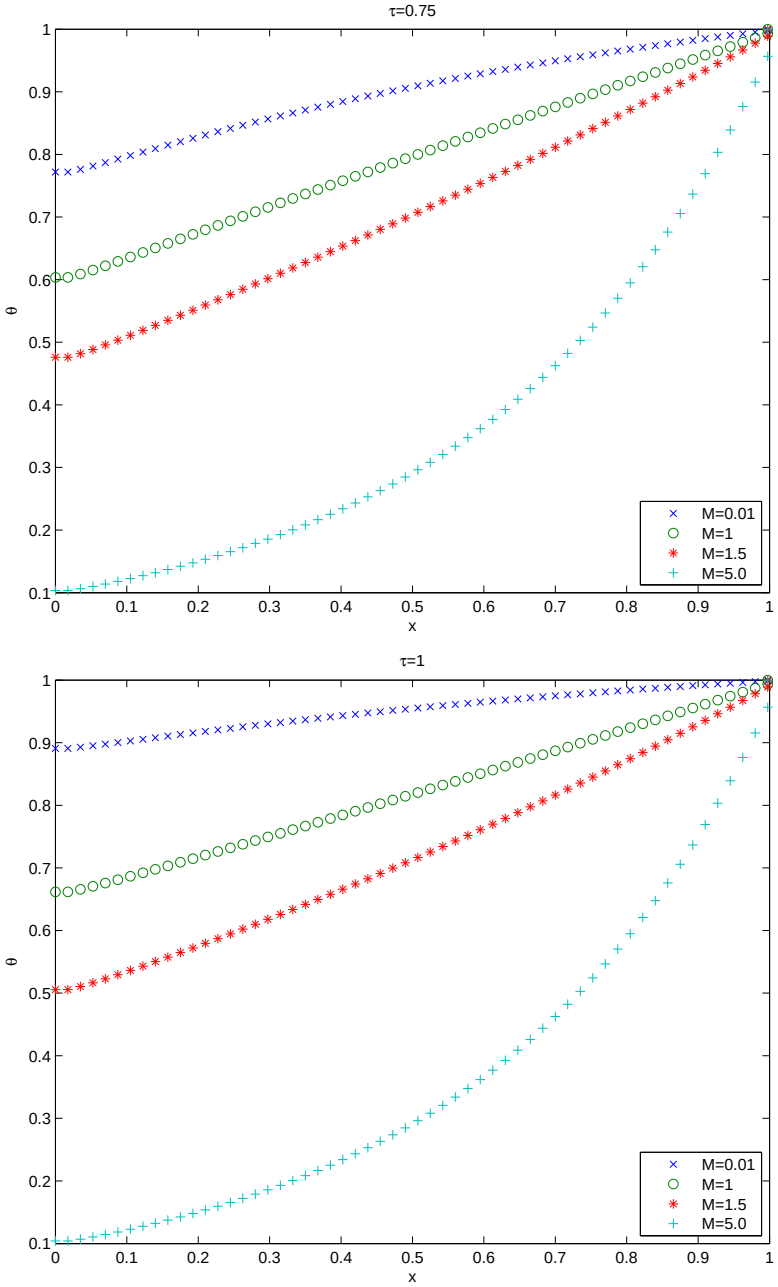

Figure 3.4: *A triangular fin profile with* $B = 1,\ n = 1,\ \mathcal{M} = 0.01,\ \mathcal{M} = 1,\ \mathcal{M} = 1.5,$ *and* $\mathcal{M} = 5$ *for* $\tau = 5(top)$ *and* $\tau = 10(bottom)$.

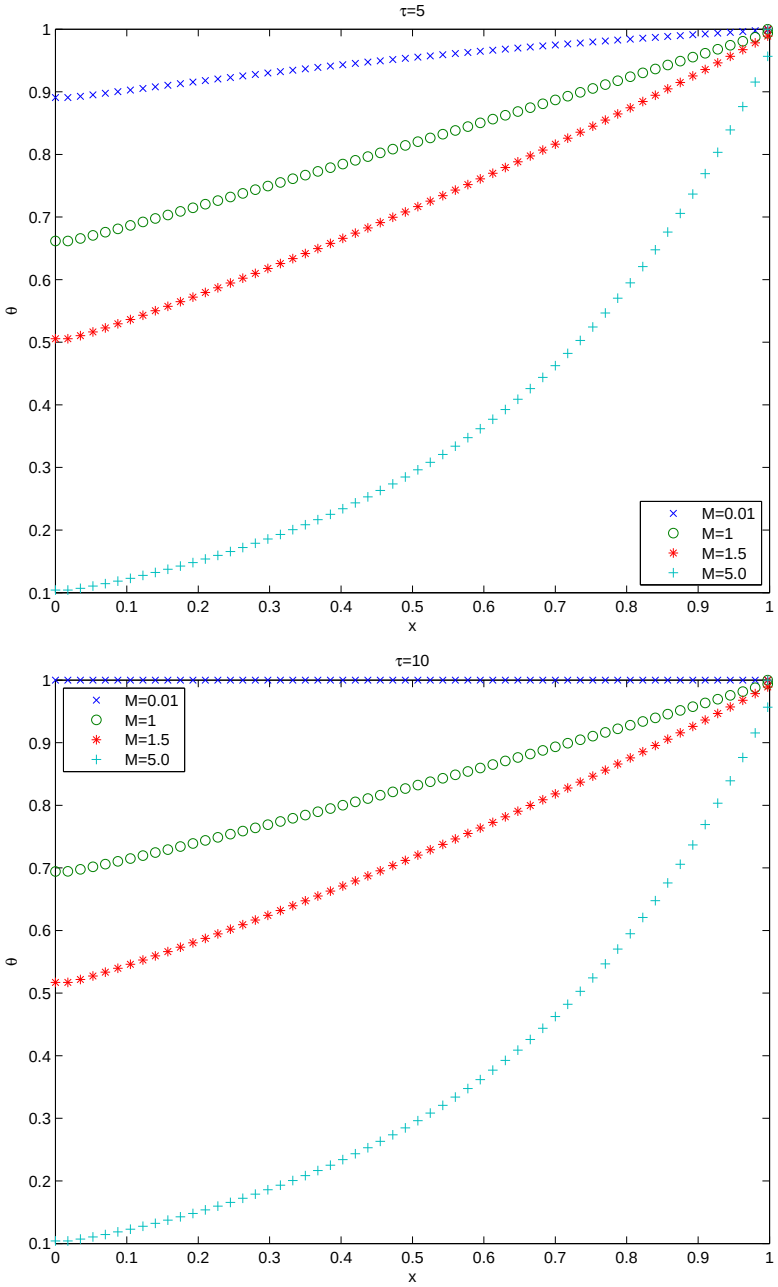

Figure 3.5: *A rectangular fin profile with* $B = 1,\ n = 1,\ \mathcal{M} = 1,\ \mathcal{M} = 3,\ \mathcal{M} = 5,$ *and* $\mathcal{M} = 8$ *for* $\tau = 2.5$

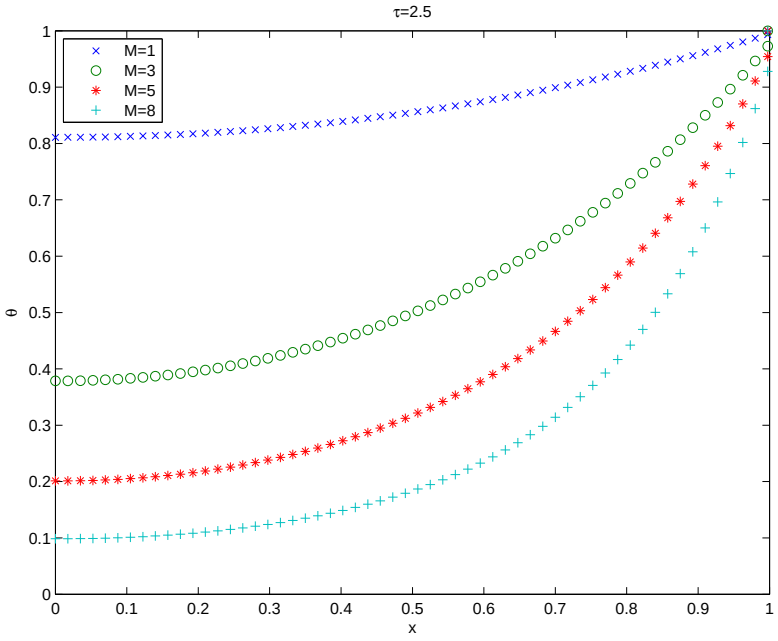

Figure 3.6: *A rectangular fin profile with* $B = 1,\ n = 1,\ \mathcal{M} = 1$ *and varying* $\tau$.

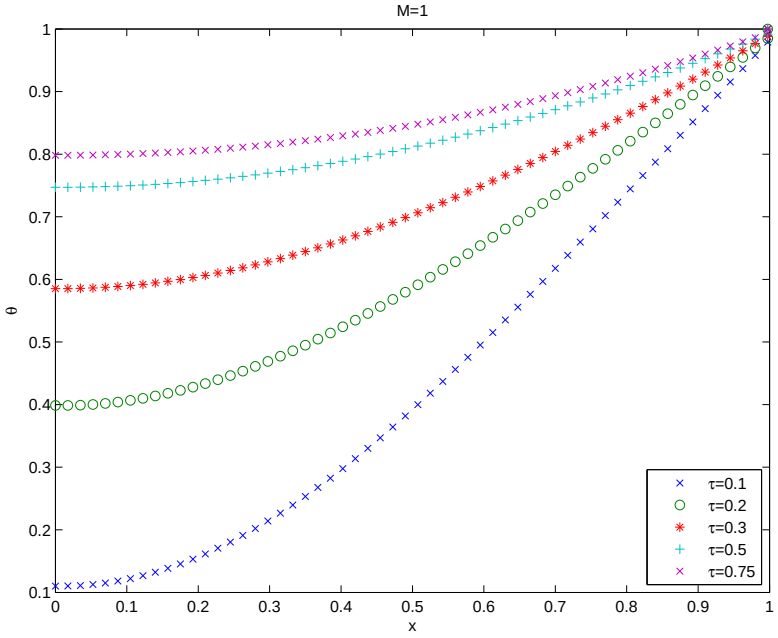


Figure 3.7: *A rectangular fin profile with* $B = 1,\ \mathcal{M} = 6,\ \tau = 2.5$ *and varying* $n$.

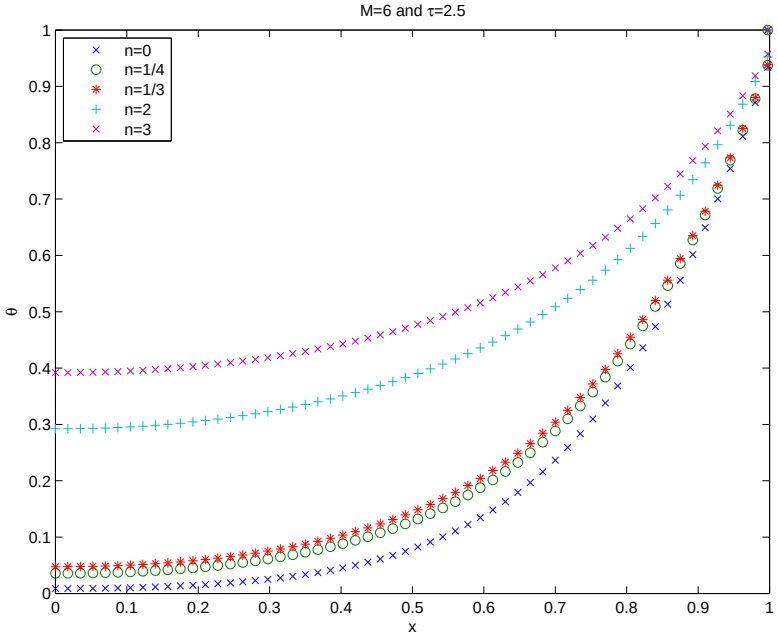

# Chapter 4

# Numerical relaxation scheme

*The work conducted in this Chapter has been published in the Journal of Applied Mathematics and Computation* [51].

## 4.1 Introduction

The analytical solution of equations of the kind as considered in this work are not easily obtained, and may often only be found through a simplification of the model. As such, given that we aim to investigate a highly non-linear partial differential equation, we will employ computational methods for the solution of the equation. Wang et al. [18] stated that one needs to treat a system of highly coupled equations with stiff non-linear source terms in the proper manner computationally so that one does not obtain spurious steady state numerical solutions - this is an appropriate consideration given the nature of the computational method we wish to employ in the Chapter. The literature [27, 52, 53] motivates the use of numerical relaxation schemes given that they are simple to implement and are able to achieve higher order accuracy in capturing weak solutions without using Riemann Solvers spatially or

systems of algebraic equations temporally. Thus we choose to establish a relaxation system for the corresponding problem under consideration. We consider the one-dimensional case, not due to its simplicity, but rather so that we are able to validate our results through a clear visualization against benchmark results. An extension to higher dimensions is straight forward given the methodology employed in this work and in [26]. Due to its robustness [53] the scheme shall be applied to the transient heat equation under consideration and as such be used to compute the mean action time for which there is no analytical technique available to us.

## 4.2 Relaxation schemes: An overview

As per the work in [54, 55], the main idea in relaxation is to avoid Riemann solvers when constructing numerical schemes for non-linear conservation laws. It is for this reason that our approach consists of reducing the order of differentiation of the heat transfer equation under consideration to a first order non-linear hyperbolic system of equations with source terms. As such, the equation considered is treated in a similar fashion to conservation laws [27, 56].

### Scalar conservation laws

To be more practical, let us take a scalar PDE or conservation law

$$u_t + [f(u)]_x = 0, \qquad x \in \mathbb{R}, \quad t \in \mathbb{R}_+, \quad u \in \mathbb{R} \tag{4.1}$$

$$u(x, 0) = u_0(x).$$

By employing the relaxation approach, equation (4.1) is transformed into a linear system of equations termed a relaxation system

$$\begin{aligned} u_t + v_x &= 0, \quad v \in \mathbb{R} \\ v_t + a u_x &= -\frac{1}{\epsilon}\left(v - f(u)\right) \\ u(x,0) &= u_0(x) \end{aligned} \tag{4.2}$$

For $\epsilon \to 0$ we have

$$v = f(u) \tag{4.3}$$

$$u_t + \left[f(u)\right]_x = 0 \tag{4.4}$$

Equation (4.4) is the original conservation law and equation (4.3) is called the local equilibrium. The parameter $\epsilon$ is called the relaxation rate and is very small while $a$ is a sub-characteristic parameter and it is always positive.

We will now introduce the Chapman-Enskog expansion as a means of deriving the relaxed schemes that have been shown to be a consistent and stable discretisation of the original conservation laws [27]. Let

$$v = v_0 + \epsilon v_1 + \epsilon^2 v_2 + .... + \epsilon^n v_n + .... \tag{4.5}$$

For $\epsilon \to 0$, the first order Chapman-Enskog expansion of $v$ is

$$v(\epsilon) = v_0(\epsilon) + \epsilon v_1. \tag{4.6}$$

Substituting the local equilibrium equation (4.3) into (4.6) we get

$$v(\epsilon) = f(u(\epsilon)) + \epsilon v_1. \tag{4.7}$$

Substituting (4.7) into the relaxation system (4.2) we get

$$\begin{aligned}
[u(\epsilon)]_t + [f(u(\epsilon))]_x + \epsilon\,[v_1(\epsilon)]_x &= 0 \\
[f(u(\epsilon))]_t + \epsilon\,[v_1(\epsilon)]_t + a\,[u(\epsilon)]_x &= \frac{1}{\epsilon}\,(f(u(\epsilon)) - v(\epsilon)) \\
&= \frac{1}{\epsilon}\,[f(u(\epsilon)) - (f(u(\epsilon)) + \epsilon v_1)] \\
&= -v_1(\epsilon)
\end{aligned} \tag{4.8}$$

that is

$$\begin{aligned}
[u(\epsilon)]_t + [f(u(\epsilon))]_x + \epsilon\,[v_1(\epsilon)]_x &= 0 \\
[f(u(\epsilon))]_t + \epsilon\,[v_1(\epsilon)]_t + a\,[u(\epsilon)]_x &= -v_1(\epsilon) \quad .
\end{aligned} \tag{4.9}$$

Equating coefficients of $\epsilon$ polynomials with the same degree we obtain

$$\begin{aligned}
[v_1(\epsilon)]_t &= 0 \\
v_1(\epsilon) &= -\,[f(u(\epsilon))]_t - a\,[u(\epsilon)]_x \quad .
\end{aligned} \tag{4.10}$$

In fact

$$[f(u)]_t = f'(u)\,[u]_t$$

and from (4.1) we have

$$[u]_t = -\,[f(u)]_x$$

and

$$[u]_t = -f'(u)\,[u]_x\,.$$

Therefore

$$[f(u)]_t = -f'(u)^2\,[u]_x \tag{4.11}$$

and by inserting (4.11) into (4.10) we obtain

$$v_1 = -\left[a - f'(u)^2\right][u]_x . \tag{4.12}$$

Given (4.12)

$$\frac{\partial v_1}{\partial x} = -\left[\left(a - f'(u)^2\right)\frac{\partial u}{\partial x}\right]_x . \tag{4.13}$$

Substituting (4.13) into the first equation of the system (4.9) we obtain

$$\frac{\partial u}{\partial t} + \frac{\partial f(u)}{\partial x} = \left[\left(a - f'(u)^2\right)\frac{\partial u}{\partial x}\right]_x \tag{4.14}$$

which is a diffusion equation. This equation physically models dissipation if

$$\left(a - f'(u)^2\right) \geq 0.$$

From this requirement we have

$$a \geq f'(u)^2$$

that is

$$\frac{f'(u)^2}{a} \leq 1$$

that is

$$\frac{|f'(u)|}{\sqrt{a}} \leq 1.$$

Therefore,

$$-\sqrt{a} \leq f'(u) \leq \sqrt{a} \tag{4.15}$$

for all $u$.

The above relation (4.15) is referred to as the sub-characteristic condition and is necessary for convergence. From Chalabi and Seghir, the sub-characteristic stability condition plays a key role and is essential to obtain zero relaxation as is the CFL condition for convergence in numerical schemes [54, 55].

## Scalar conservation laws with source term

In order to tackle our problem we need to first consider the structure of conservation laws with source terms. The approach employed follows the work of Chalabi and Seghir [55]. The general problem is expressed by the following equations

$$u_t + [f(u)]_x = q(u), \qquad x \in \mathbb{R}, \quad t \in \mathbb{R}_+, \quad u \in \mathbb{R} \tag{4.16}$$

$$u(x,0) = u_0(x).$$

From equation (4.16), the corresponding relaxation system is given by

$$\begin{aligned} u_t + v_x &= q(u), \quad v \in \mathbb{R} \\ v_t + a u_x &= -\frac{1}{\epsilon}\left(v - f(u)\right) \\ u(x,0) &= u_0(x). \end{aligned} \tag{4.17}$$

For $\epsilon \to 0$ we have

$$v = f(u) \tag{4.18}$$

$$u_t + [f(u)]_x = q(u). \tag{4.19}$$

Equation (4.19) is the original conservation law and equation (4.18) is called the local equilibrium. By the Chapman-Enskog approximation, the first order approximation of the relaxation system becomes

$$\frac{\partial u}{\partial t} + \frac{\partial f(u)}{\partial x} = q(u) + \epsilon\left[f'(u)q(u)\right]_x + \epsilon\left[\left(a - f'(u)^2\right)\frac{\partial u}{\partial x}\right]_x \tag{4.20}$$

which is dissipative if

$$-\sqrt{a} \le f'(u) \le \sqrt{a} \tag{4.21}$$

for all u.

The sub-characteristic condition is similar to that obtained for homogeneous conservation laws.

Employing the relaxation technique is quite straight forward at this stage. Transformations are used as a means of reducing the order of differentiation by one as per the work in [29, 57]. After appropriate transformations, we obtain an equation in the form of a conservation law with a source term. Relaxation techniques can be employed as per the work of Chalabi and Seghi [54]. In the next Section, an upwind scheme is considered as an alternative means of solving our problem. This method is appropriate given that Jin and Xin [27] described them as schemes having a correct zero relaxation limit.

## 4.3 Numerical relaxation scheme for one dimensional heat transfer

The relaxation scheme is structured via the introduction of a linear system with source term. We consider

$$\frac{\partial \theta}{\partial \tau} = \frac{\partial}{\partial x}\left(f(x)k(\theta)\frac{\partial \theta}{\partial x}\right) - \mathcal{M}^2\theta^{n+1}, \qquad 0 < x < 1, \quad \tau \geq 0 \tag{4.22}$$

where boundary conditions are as follows

$$\frac{\partial \theta}{\partial x}\Big|_{x=0} = 0 \quad \text{at the fin tip} \quad \text{and} \quad \theta(\tau, 1) = 1. \tag{4.23}$$

The corresponding relaxation system is

$$\begin{aligned} \frac{\partial \theta}{\partial \tau} + \frac{\partial v}{\partial x} &= -\mathcal{M}^2 \theta^{n+1} \\ \frac{\partial v}{\partial \tau} + a^2 \frac{\partial \theta}{\partial x} &= \frac{1}{\epsilon}(F - v) \\ \frac{\partial \theta}{\partial x}\Big|_{x=0} = 0 \qquad & and \quad \theta(\tau, 1) = 1 \\ v(\tau, 0) = F(0) = 0 \quad & and \quad v(\tau, 1) = F(1) \end{aligned} \quad . \tag{4.24}$$

with $F = -f(x)k(\theta)\dfrac{\partial \theta}{\partial x}$, $a$ the characteristic speed and $\epsilon$ the relaxation parameter. The key concept of this theory is that the relaxation system should reduce to (4.22) for $\epsilon \mapsto 0$ and the partial differential operator of the relaxation system is linear and diagonalizable with two characteristics

$$v \pm a\theta.$$

With this approach, special care should be taken when discretising the system (4.24) so that there is still a discrete analogy for the zero relaxation limit which is consistent with the original equation (4.22).

### 4.3.1 Numerical discretisation

In order to discretise the spatial grid we define the points $x_{i+\frac{1}{2}}$ with mesh width $\Delta x_i = x_{i+\frac{1}{2}} - x_{i-\frac{1}{2}}$ as well as the time step $\Delta \tau_j = \tau_{j+1} - \tau_j$ such that $\theta_i^j$ denotes the approximation cell average of $\theta$ in the cell $\left[x_{i-\frac{1}{2}}, x_{i+\frac{1}{2}}\right]$ at time $\tau_j$ while $\theta^j_{i+\frac{1}{2}}$ is the approximation of $\theta$ at $x = x_{i+\frac{1}{2}}$ and $\tau = \tau_j$.

**Relaxation scheme**

Using the integral approach and spatial cell averaging of equation (4.24) we get

$$\begin{aligned} \frac{d\theta_i}{d\tau} + \frac{1}{\Delta x_i}\left(v_{i+\frac{1}{2}} - v_{i-\frac{1}{2}}\right) &= -\mathcal{M}^2\theta_i^{n+1} \\ \frac{dv_i}{d\tau} + a^2\frac{1}{\Delta x_i}\left(\theta_{i+\frac{1}{2}} - \theta_{i-\frac{1}{2}}\right) &= \frac{1}{\epsilon}\left(F_i - v_i\right) \\ \frac{1}{\Delta x_i}\int_{x_{i-\frac{1}{2}}}^{x_{i-\frac{1}{2}}} F(\theta)dx + o\left(\Delta x^2\right) &= F_i \end{aligned} \tag{4.25}$$

as established and similarly defined by Jin and Xin [27]. By employing an upwind scheme, quantities $\theta_{i+\frac{1}{2}}$ and $v_{i+\frac{1}{2}}$ are easily defined. This is due to the fact that the system (4.24) has two characteristic variables $v \pm a\theta$ travelling with characteristic speeds $\pm a$ respectively. Hence

$$(v + a\theta)_{i+\frac{1}{2}} = (v + a\theta)_i \tag{4.26}$$

$$(v - a\theta)_{i+\frac{1}{2}} = (v - a\theta)_{i+1}\,. \tag{4.27}$$

From (4.26) we get

$$v_{i+\frac{1}{2}} + a\theta_{i+\frac{1}{2}} = v_i + a\theta_i \tag{4.28}$$

and from (4.27) we get

$$v_{i+\frac{1}{2}} - a\theta_{i+\frac{1}{2}} = v_{i+1} - a\theta_{i+1}. \tag{4.29}$$

By adding (4.28) with (4.29) and after some algebraic manipulation we obtain

$$v_{i+\frac{1}{2}} = \frac{1}{2}\left(v_i + v_{i+1}\right) - \frac{a}{2}\left(\theta_{i+1} - \theta_i\right). \tag{4.30}$$

Similarly, by subtracting (4.29) from (4.28) we find

$$\theta_{i+\frac{1}{2}} = \frac{1}{2}\left(\theta_i + \theta_{i+1}\right) - \frac{1}{2a}\left(v_{i+1} - v_i\right). \tag{4.31}$$

From equation (4.30) and (4.31) we obtain the following important expressions

$$v_{i+\frac{1}{2}} - v_{i-\frac{1}{2}} = \frac{1}{2}\left(v_{i+1} - v_{i-1}\right) - \frac{a}{2}\left(\theta_{i+1} - 2\theta_i + \theta_{i-1}\right) \tag{4.32}$$

and

$$\theta_{i+\frac{1}{2}} - \theta_{i-\frac{1}{2}} = \frac{1}{2}\left(\theta_{i+1} - \theta_{i-1}\right) - \frac{1}{2a}\left(v_{i+1} - 2v_i + v_{i-1}\right). \tag{4.33}$$

By introducing equations (4.32) and (4.33) into the system (4.25) we finally obtain a relaxing scheme as expressed by the system

$$\begin{aligned}
\frac{d\theta_i}{d\tau} &= -\frac{1}{2\Delta x_i}\left(v_{i+1} - v_{i-1}\right) + \frac{a}{2\Delta x_i}\left(\theta_{i+1} - 2\theta_i + \theta_{i-1}\right) - \mathcal{M}^2\theta_i^{n+1} \\
\frac{dv_i}{d\tau} &= \frac{-a^2}{2\Delta x_i}\left(\theta_{i+1} - \theta_{i-1}\right) + \frac{a}{2\Delta x_i}\left(v_{i+1} - 2v_i + v_{i-1}\right) + \frac{1}{\epsilon}\left(F_i - v_i\right) \\
F_i &= f(x_i)k(\theta_i)\frac{\theta_{i+1} - \theta_{i-1}}{2\Delta x_i}
\end{aligned} \tag{4.34}$$

for the one dimensional heat transfer equation under consideration.

### 4.3.2 Zero relaxation numerical scheme

When structuring the relaxation scheme it was required that the numerical discretisation must have a discrete analogy to the zero relaxation limit which should be consistent with the original partial differential equation. In our case, for $\epsilon \to 0$, we have $v_i \to F_i$ and hence the zero relaxation numerical scheme becomes

$$\begin{aligned}
\frac{d\theta_i}{d\tau} &= -\frac{1}{2\Delta x_i}\left(F_{i+1} - F_{i-1}\right) + \frac{a}{2\Delta x_i}\left(\theta_{i+1} - 2\theta_i + \theta_{i-1}\right) - \mathcal{M}^2\theta_i^{n+1} \\
F_i &= f(x_i)k(\theta_i)\frac{\theta_{i+1} - \theta_{i-1}}{2\Delta x_i} \\
F_0 &= 0.
\end{aligned} \tag{4.35}$$

Hence the first order fully discretized scheme can be expressed as

$$\begin{aligned} \theta_i^{j+1} &= \theta_i^j - \frac{\Delta\tau}{2\Delta x_i}\left(F_{i+1} - F_{i-1}\right) + \frac{a\Delta\tau}{2\Delta x_i}\left(\theta_{i+1} - 2\theta_i + \theta_{i-1}\right) - \Delta\tau\mathcal{M}^2\theta_i^{n+1} \\ F_0 &= 0. \end{aligned} \tag{4.36}$$

The above expression stands for a relaxed numerical scheme for heat transfer in one dimensional longitudinal fin profile. In this research we will test this scheme via a comparison against analytical solutions of the steady state equation solved by Turkyilmazoglu [30].

## 4.4 Results and discussion

### 4.4.1 Parametric exponential shape profiles and model validation

We consider equation (4.22) and define the fin profile as a parametric exponential profile. We note here that in the context of this Chapter and throughout the rest of the thesis reference to an 'exponential fin' or 'exponential fin profile(s)' serve as a means of easily distinguishing between fins with an exponential shape function $e^{\alpha x}$ and those with other shape functions. We note here that for $\alpha > 0$ Kraus et al. [11] referred to this shape as the 'convex fin'. Given this choice of the fin shape profile and the thermal conductivity as a power law it follows that

$$f(x) = e^{\alpha x},$$

and

$$k(\theta) = \theta^m$$

Figure 4.1: *Temperature distribution for a rectangular fin profile where* $\alpha = 0$ *(top) and an exponential fin profile* $\alpha = 1$ *(bottom) with* $n = m = 1/4$ *obtained via the relaxation scheme (____) compared to a steady state solution (∘ ∘ ∘∘).*

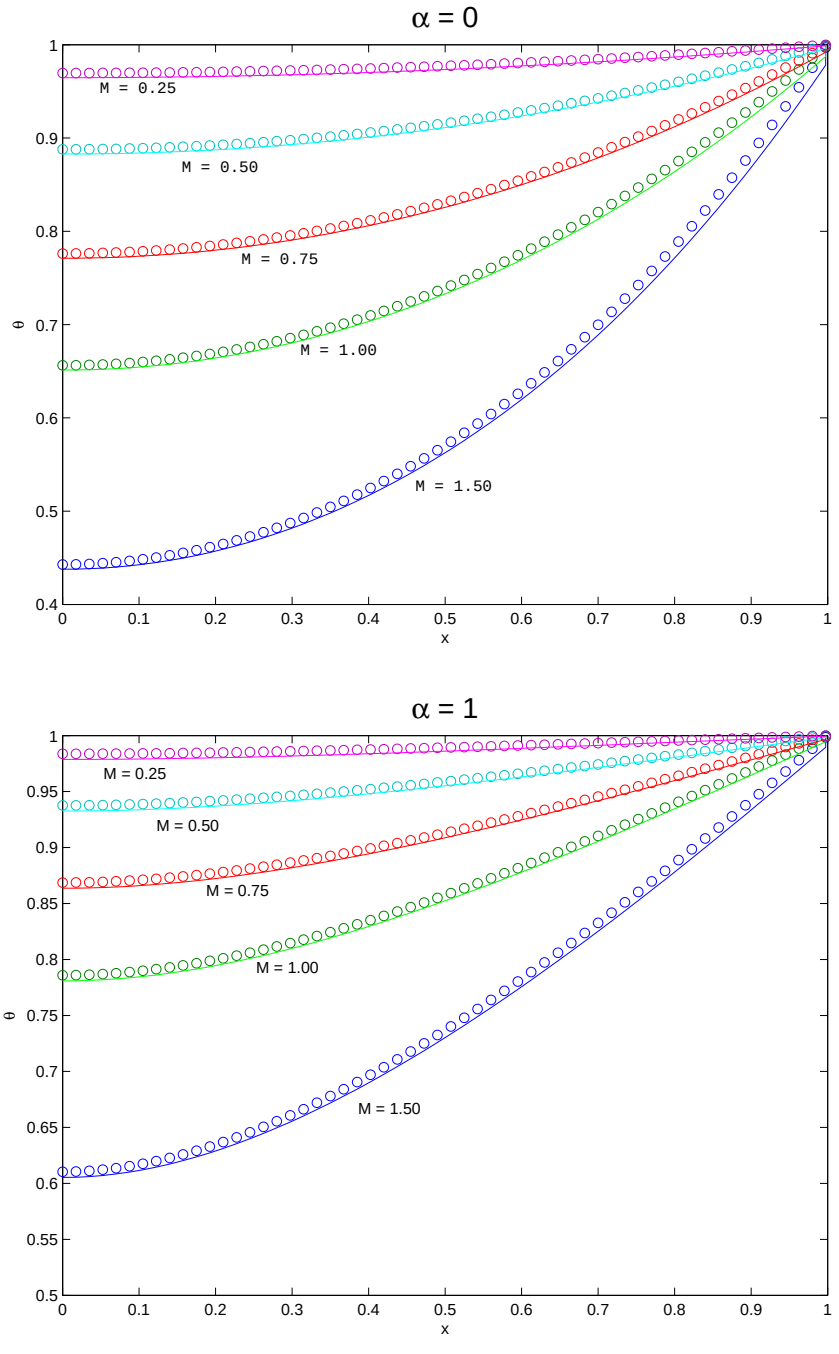

Figure 4.2: *Temperature distribution for an exponential fin profile where* $\alpha = 2$ *(top) and* $\alpha = 3$ *(bottom) with* $n = m = 1/4$ *obtained via the relaxation scheme (____) compared to a steady state solution (○ ○ ○○).*

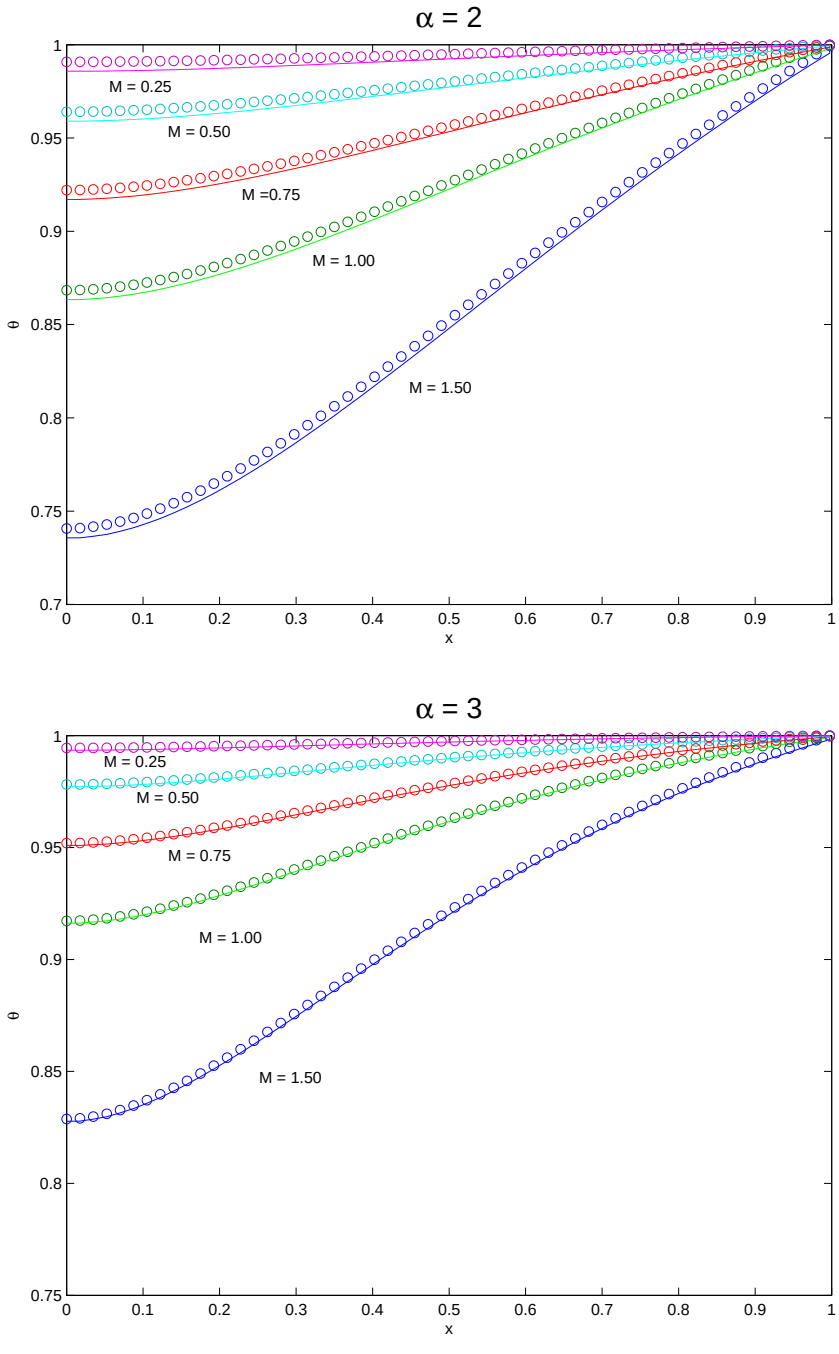

which gives

$$\frac{\partial \theta}{\partial \tau} = \frac{\partial}{\partial x}\left(e^{\alpha x}\theta^m \frac{\partial \theta}{\partial x}\right) - \mathcal{M}^2\theta^{n+1}, \qquad 0 < x < 1, \quad \tau \geq 0 \tag{4.37}$$

where the boundary conditions are as follows

$$\frac{\partial \theta}{\partial x}\Big|_{x=0} = 0 \qquad \text{at the fin tip.} \tag{4.38}$$

In this research we have chosen to consider a fin with exponential profile which reduces to the rectangular profile when $\alpha = 0$. This problem has been solved analytically for steady states [30] and as such we use those results to validate our numerical relaxation scheme. While analytical solutions do exist for steady states [30], it is difficult to obtain such solutions for the time dependent case of equation (4.37). In this Section we consider the heat flow in one dimensional exponential fins with varying values of the exponential parameter, thermo-geometric parameter and nonlinear thermal conductivity exponent. In much research regarding heat transfer, rectangular fins are often considered when multiple numerical and analytical methods are employed [1, 46, 58]. In addition, exact analytical solutions are available for the steady state equation of heat transfer in straight fins of exponential shape [30]. Therefore, we consider these fin shapes in the transient case so as to better validate our numerical results. We obtain numerical solutions via the relaxation scheme and then discuss the results. The variation of the exponential parameter is essential as it allows us to consider different profiles, one of which is the rectangular profile when $\alpha = 0$, allowing for a comparison to analytical steady state solutions. In order to compute steady state solutions from the time dependent model, we allow our numerical solutions to converge over large time to within a certain tolerance. In this manner we are able to compare our numerical solutions to steady state solutions established analytically by Turkyimazoglu [30]. Figures 4.1 and 4.2 depict analytical steady state solutions ($\circ\ \circ\ \circ\ \circ\ \circ$) as well

as the time dependent numerical solutions (_____) at $\mathcal{M} = 0.25, 0.5, 0.75, 1.00$ and 1.50. These Figures show that the numerical relaxation results of the transient heat equation converges reasonably well to the analytical solutions from the steady state heat equation. As such, our numerical results have been validated via the comparison, allowing us to assume that using the same scheme to compute the mean action time is reasonable.

### 4.4.2 Temperature distribution and fin efficiency

In our figures we have compared the analytical solution of the steady state case to our numerical solutions for the rectangular case and the cases where $\alpha = 1, 2, 3$ and 4. This was used to highlight how the temperature distribution increases with the increase of the parameter $\alpha$ and hence to show that the fin performance, in terms of a high heat distribution, becomes better with the parameter increase. For each case, we vary $\mathcal{M}$ to better compare our results across different fin lengths as well - it has been shown by Harley [59] that $\mathcal{M}$ is proportional to the fin length allowing for this approach. From Figures 4.1 and 4.2 it is clear that the temperature distribution decreases as one moves along the fin from the base to the tip. Furthermore, we find that the overall temperature distribution is higher for larger values of the fin shape parameter $\alpha$ which complies with [30]. The temperature distribution is also shown to be higher across the fin length the shorter the fin which complies with the idea that short fins shall transfer heat quicker than long fins with similar properties as per the work of Moitsheiki and Harley [1].

## 4.5 Conclusion

In this Section, we have used a numerical relaxation scheme to solve a time dependent one dimensional heat transfer equation with different exponential fin profiles. The numerical relaxation scheme was implemented due to its simplicity and accuracy as described in the literature by Jin and Xin [27]. To the best of the authors' knowledge this is the first time that this method has been employed within the context of such a problem. The results obtained complied with steady state analytical solutions [30] upon computational convergence. As such we are able to use this scheme to further investigate the mean action time of the process, as we will discuss in Chapter 6.

# Chapter 5

# Comparison of numerical schemes

## 5.1 Introduction

It is important to compare results from different utilized methods, not necessarily with each other, but more importantly with some known analytical or semi-analytical solution as a means of investigating their efficiency. We paraphrase Tadman [60] who explained that there does not necessarily exist a "best" numerical method but rather that each method of particular interest is used within a context and will display its own strengths and weaknesses. Therefore, neither the numerical well-balanced scheme nor the numerical relaxation scheme should be considered the best scheme to use for the solution of the non-linear heat transfer equation under consideration since each method has its own advantages and disadvantages. As stipulated in the Introduction the methods employed have certain strengths which is why we have employed them in this work. While standard finite difference schemes may also perform sufficiently we employed these methods with the express intention of applying the adiabatic boundary condition in the appropriate fashion.

The true motivation for the use of the methods employed here is due to the work conducted in [1] where it was found that the results obtained were not maintaining the physical conditions for singular fins. The idea was to use an integral approach method such as the Finite Volume Method since it reduces the order of differentiation by one through the Gauss divergence theorem. The well-balanced and relaxation methods are applied via the FVM allowing each to take advantage of the latter's advantages. Given each method's particular advantages as discussed in the Introduction and Chapters 3 and 4 their use is justified. Therefore, the next Section consists in comparing the results obtained in these Chapters as well as drawing some conclusions regarding their performance.

## 5.2 Comparison and convergence of numerical schemes

Since numerical schemes produce only approximations to the exact solution of a relevant PDE an investigation into the stability, consistency and convergence of the scheme is of prime importance. Unfortunately, we are dealing with a non-linear PDE which means that investigations into the stability can become extremely complex. Given that the consistency, i.e. the order of accuracy of the schemes are well known via the finite difference approximations employed, we will focus on a convergence analysis in this Chapter. As such, we shall compare the numerical results to the exact solution for the following particular case of

$$\frac{\partial \theta}{\partial t} - \frac{\partial^2 \theta}{\partial x^2} = -\mathcal{M}^2 \theta. \tag{5.1}$$

where initial and boundary conditions are given as

$$\theta(x, 0) = 0$$

$$\frac{\partial \theta}{\partial x}(0,\tau) = 0,\ \tau > 0$$

and

$$\theta(1,\tau) = 1,\ \tau > 0.$$

As a linear PDE, an analytical solution is straight forward and well known [24]. In addition, we will also consider different cases for the PDE which models fins with an exponential profile since its steady state equation modelled by

$$\frac{d}{dx}\left(e^{(\alpha x)}\theta^m \frac{d\theta}{dx}\right) = \mathcal{M}^2\theta^{n+1}, \quad 0 \leq x \leq 1 \tag{5.2}$$

$$\frac{d\theta}{dx}(0) = 0; \qquad \theta(1) = 1$$

admits some analytical solutions [30]. These analytical solutions will be used as a benchmark for our numerical solutions as a means of discussing the convergence of these schemes.

### 5.2.1 Convergence for small $\tau$

Establishing the convergence of many non-linear problems is not always a simple matter. In fact, unlike many linear differential equations, there is no well established approach which can be used to analyse the convergence of numerical methods for non-linear PDEs [60]. The challenges vary from problem to problems and the specific characteristics of the non-linearity. Also, here are certain requirements regarding the norms to be employed in order to enforce compactness. So, matching these norms to initial boundary values coupled with the non-linearity is a delicate task and sometimes impossible to prove analytically.

Figure 5.1: *Exact solutions for* $M = 0.5$, *at* $\tau = 0.0005$; $\tau = 0.001$; $\tau = 0.005; \tau = 0.01$.

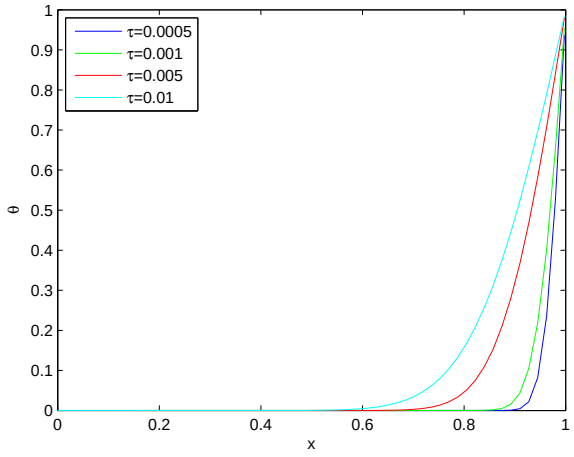


In this Section, we shall present the results of equation (5.1) obtained via the numerical well-balanced and relaxation schemes, compare their results and compute the errors with respect to the exact solutions and discuss the convergence. In all numerical computations we have taken $\Delta\tau = 10^{-5}$ and $\Delta x = 1.75 \times 10^{-2}$ and the use of $\tau$ refers to the final time at which a numerical solution is presented.

At first glance - see Figures 5.1 and 5.2 - it would seem that there are differences between the exact solution to equation 5.1 and the numerical solutions obtained via our two schemes. However, to quantitatively represent this we have computed the mean square errors for the well-balanced and relaxation schemes against the exact solution and displayed this information in Table 5.1 where the second column represents the comparison with the well-balanced numerical scheme, the third column represents the comparison with the relaxation scheme and the last column represents the mean square error between the well-balanced and relaxation schemes. At this

Figure 5.2: *Numerical well-balanced (∘ ∘ ∘∘) and relaxation (___) solutions for* $M = 0.5$*, at* $\tau = 0.0005$; $\tau = 0.001$; $\tau = 0.005$; $\tau = 0.01$.

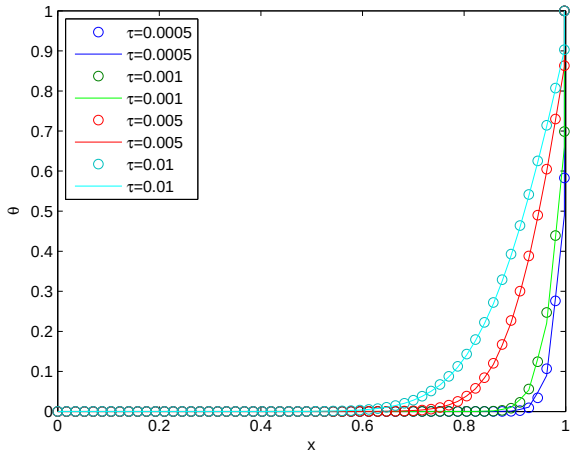


stage we also note that we have considered various values of $\tau$ as a means of asserting the time taken to convergence as well.

In Table 5.1 we can see that the schemes employed in Chapters 3 and 4 converge to the exact solution to two decimal places for small values of $\tau$. This makes sense given the order of accuracy of the schemes employed having been of second order. We also notice that as $\tau$ increases the errors between the numerical solutions and the exact solutions decrease and as such we find the former are accurate to within three decimal places. This confirms that our numerical schemes perform more accurately for larger values of $\tau$ which is not unreasonable. Furthermore, we find that there is a negligible difference between the two schemes for these values of $\tau$ which indicates that the two schemes are on par in terms of their performance in terms of convergence.

For large values of $\tau$, the steady state solutions are more appropriate to use as a

Table 5.1: *Mean squared error obtained via a comparison between the steady state solution and our numerical solutions; and the mean squared difference between the two schemes for small values of* $\tau$

| $\tau$ | WBS | RS | WBS vs RS |
|---|---|---|---|
| 0.0005 | 0.0036 | 0.0048 | 0.0002 |
| 0.001 | 0.0025 | 0.0031 | 0.0000 |
| 0.005 | 0.0011 | 0.0012 | 0.0000 |
| 0.01 | 0.0007 | 0.0008 | 0.0000 |

benchmark. As such we now turn to the work of Turkyilmazoglu [30] who has obtained exact solutions of the steady state equation given by equation (5.2).

### 5.2.2 Convergence for large $\tau$

In this Subsection we present a comparison between the well-balanced scheme, the relaxation scheme and a steady state solution respectively. We consider the following equation as a means of investigating the convergence of our numerical schemes

$$\frac{\partial \theta}{\partial \tau} = \frac{\partial}{\partial x}\left(\theta^m \frac{\partial \theta}{\partial x}\right) - \mathcal{M}^2 \theta^{n+1}, \quad 0 < x < 1, \quad \tau \geq 0 \tag{5.3}$$

where the initial and boundary conditions are as follows

$$\frac{\partial \theta}{\partial x}\Big|_{x=0} = 0 \quad \text{at the fin tip,} \quad \theta(1,\tau) = 1 \quad \text{and} \quad \theta(x,0) = 0, \tag{5.4}$$

where $m = n = 1/4$. This equation has steady state solutions as stated in [30]. The error between this steady state solution and the solutions computed via the different numerical schemes employed for equation (5.3) are presented below for different values of $\mathcal{M}$. We have also provided the values of $\tau$ at which the value of the numerical solution was obtained in each case.

Table 5.2: *Mean squared error obtained via a comparison between the steady state solution and our numerical solutions; and the mean squared difference between the two schemes for* $\tau = 0.01$

| $\mathcal{M}$ | WBS | RS | WBS vs RS |
|---|---|---|---|
| 0.01 | 0.8500 | 0.8497 | 0.0001 |
| 0.5 | 0.7124 | 0.7120 | 0.0000 |
| 1.5 | 0.2882 | 0.2879 | 0.0000 |
| 5 | 0.0296 | 0.0294 | 0.0000 |

Firstly we can see that the solutions to both schemes start to converge at relatively small values of $\tau$ - compare Tables 5.2 and 5.3. It becomes clear from Tables 5.3 and 5.4 that both numerical schemes converge at least up to two decimal places, which is consistent with the accuracy of the finite difference approximations employed. By

Table 5.3: *Mean square error obtained via a comparison between the steady state solution and our numerical solutions; and the mean squared difference between the two schemes for* $\tau = 1$

| $\mathcal{M}$ | WBS | RS | WBS vs RS |
|---|---|---|---|
| 0.01 | 0.0071 | 0.0084 | 0.0001 |
| 0.5 | 0.0038 | 0.0044 | 0.0000 |
| 1.5 | 0.0002 | 0.0002 | 0.0000 |
| 5 | 0.0005 | 0.0004 | 0.0000 |

the point at which $\tau = 5$ sufficient convergence has been reached over various values of $\mathcal{M}$. In principle, the steady state solution is reached when $\tau$ is relatively large and as such taken to be infinity. Furthermore, we note that for smaller values of $\mathcal{M}$ convergence can be up to four decimal places. As $\mathcal{M}$ increases we find that the error between the computational solutions and the steady state solutions increase, indicating the impact of the approximations employed on the non-linear term.

As a result, it can clearly be seen that the numerical solutions follow to the physical behaviour of transient heat transfer and verify the results of the literature [11, 24, 30]. This is indicative of the efficiency and appropriateness of the schemes employed. Furthermore, we can also strengthen our claims at convergence by considering the fact that, as per [26, 62], the temperature distribution is an increasing function for both

Table 5.4: *Mean squared error obtained via a comparison between the steady state solution and our numerical solutions; and the mean squared difference between the two schemes for* $\tau = 5$

| $\mathcal{M}$ | WBS | RS | WBS vs RS |
|---|---|---|---|
| 0.01 | 0.0000 | 0.0000 | 0.0000 |
| 0.5 | 0.0000 | 0.0000 | 0.0000 |
| 1.5 | 0.0001 | 0.0001 | 0.0000 |
| 5 | 0.0005 | 0.0004 | 0.0000 |

$x$ and $\tau$. Our numerical results have shown that they obey the same behaviour and are bounded by the steady state solutions. It is known that any monotonically bounded sequence converges [61] and this is the case here. Unfortunately, due to the non-linear term in the equation it is not a simple exercise to prove convergence in a theoretical fashion and as such we have provided computational justification instead.

## 5.3 Conclusion

The numerical well-balanced and relaxation schemes have been compared to analytical solutions as a means of investigating their convergence. We have tested numerically whether the obtained results converge to the true solutions for both small and large values of time. The non-linearity of the equation under consideration limits our

Figure 5.3: *Steady state solution for* $m = n = 1/4$, $M = 0.01$; $M = 0.5$; $M = 1.5$; $M = 5$

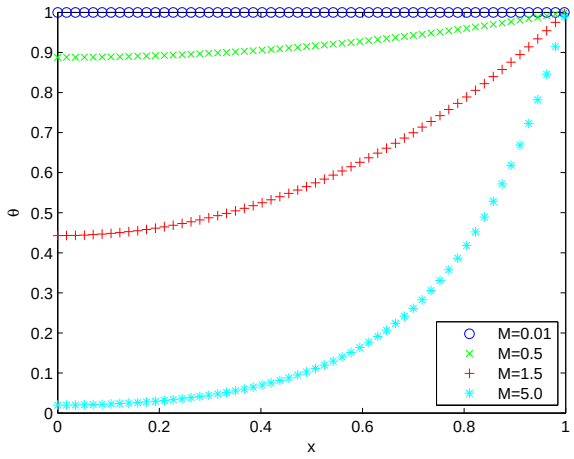


Figure 5.4: *Well-balanced and relaxation results for* $\tau = 5$, $m = n = 1/4$, $M = 0.01$; $M = 0.5$; $M = 1.5$; $M = 5$

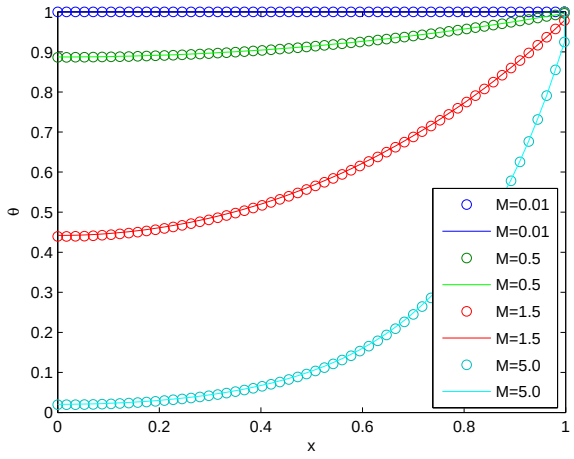

ability to investigate convergence in an analytical fashion and as such this remains to be done. However, our results have confirmed the efficiency and appropriateness of the numerical schemes employed. As such, our choices have justification and provide us with comfort regarding their usefulness in the solution of equations of the form considered in this thesis.

# Chapter 6

# Mean action time

*The work conducted in this Chapter has been published in the Journal of Applied Mathematics and Computation* [51].

## 6.1 Introduction

A common concern in heat transfer is the time taken by the process to reach a specific state when initial and limited boundary information is provided. However, it is more complex when the governing equation is non-linear such as is the case in this thesis. Complications arise not only due to the non-linearity of the equation, but also due to the fact that it is unknown at what temperature the steady state has been reached. In heat transfer this is frequently the case. McNabb and Wake [31] and McNabb [32] suggested that to compute the averaged quantity known as the mean action time may be a more realistic approach to gaining such information. This approach can easily be applied to scenarios with special boundary values providing the final state. In our case however, we do not have such information and as such we approach the problem differently.

## 6.2 Particle lifetime: Similar insights

Any transition process from a temperature $\theta_i$ to a steady state temperature $\theta_s$ is associated with a finite transition time $t_s$. It is very important to point out that this process is similar in nature to the decay time of a disintegrating particle [31]. Let $m(t)$ be the mass of the matter at time $t$ satisfying

$$\frac{dm}{dt} = -\lambda m. \tag{6.1}$$

Hence

$$m = m_0 e^{-\lambda t} \tag{6.2}$$

where $m$ decays exponentially such that for $t \to \infty$, $m \to 0$. In the field of life science, it is common to ask questions such as how long does it take for a particle of mass $m_0$ at the beginning to reach its half mass. The answers are obtained from a very simple algebraic manipulation, however we recall it here to better prepare the ground work of the next Section. For $m = \frac{m_0}{2}$ we have

$$\frac{m_0}{2} = m_0 e^{-\lambda t}$$

that is

$$\frac{1}{2} = e^{-\lambda t}$$

such that

$$ln(2) = \lambda t.$$

If we call this time $t_{\frac{1}{2}}$ we obtain

$$t_{\frac{1}{2}} = \frac{ln(2)}{\lambda}.$$

The question which comes to mind is why $t_{\frac{1}{2}}$ and not any other particular moment? As an alternative methodology, one can rather consider the mean particle lifetime

that can be sketched via a probabilistic path approach. In this way we have

$$t_{mean} = \int_0^\infty tJ(t)dt \tag{6.3}$$

with $J(t)$ an associated density function. Let $c$ be the normalizing factor to convert this quantity to a probability density function. Then

$$\int_0^\infty cm_0 e^{-\lambda t}dt = 1$$

and

$$c = \frac{1}{\int_0^\infty m_0 e^{-\lambda t}dt} \tag{6.4}$$

or

$$c = \frac{\lambda}{m_0}.$$

Therefore,

$$J(t) = \lambda e^{-\lambda t}. \tag{6.5}$$

Then, substituting (6.5) into (6.3) we obtain the particle mean lifetime as computed here bellow

$$\begin{aligned} t_{mean} &= \int_0^\infty t\lambda e^{-\lambda t}dt \\ &= \frac{1}{\lambda}. \end{aligned} \tag{6.6}$$

Alternatively, using (6.2) in (6.4) we obtain

$$c = \frac{1}{\int_0^\infty mdt} \tag{6.7}$$

and incorporating (6.1) into (6.7) leads to

$$c = \frac{\lambda}{\int_0^\infty \frac{-dm}{dt}dt} \tag{6.8}$$

Hence the probability density generated is then

$$J(t) = cm_0 e^{-\lambda t}$$

$$= cm(t) \tag{6.9}$$

$$= c\left(\frac{-1}{\lambda}\frac{dm}{dt}\right) \quad .$$

From (6.8) and (6.9) the generated probability density becomes

$$J(t) = \frac{\left(-\frac{dm}{dt}\right)}{\int_0^\infty \left(-\frac{dm}{dt}\right) dt}. \tag{6.10}$$

Therefore, the mean time shall be expressed by

$$t_{mean} = \frac{\int_0^\infty t\left(-\frac{dm}{dt}\right) dt}{\int_0^\infty \left(-\frac{dm}{dt}\right) dt}. \tag{6.11}$$

It is straight forward to confirm results obtained in (6.6) by using (6.11).

In fact,

$$\int_0^\infty t\frac{dm}{dt}dt = tm|_0^\infty - \int_0^\infty mdt$$

$$= o - \int_0^\infty mdt \tag{6.12}$$

$$= \frac{1}{\lambda}\int_0^\infty \frac{dm}{dt}dt.$$

Substituting (6.12) into (6.11) we obtain

$$t_{mean} = \frac{1}{\lambda}. \tag{6.13}$$

Therefore, the transition mean time is provided by

$$t_{mean} = \frac{\int_0^\infty t\frac{dm}{dt}dt}{\int_0^\infty \frac{dm}{dt}dt}. \tag{6.14}$$

As stated previously, the same idea can be extended to the heat transfer transition time computation as introduced by McNabb and Wake [31].

## 6.3 Numerical Mean Action Time

Landman and McGuiness [33] explain that because diffusive processes often take an infinite amount of time to come to equilibrium it is much simpler and more convenient to consider an averaged time. Thus, given that we do not know what the final steady state temperature is, the best approach to use for a non-linear heat transfer problem with temperature dependent thermal conductivity is to consider the mean average time instead as a measure for when the process has reached some kind of equilibrium. From the energy balance for a one dimensional fin we have

$$\frac{\partial \theta}{\partial \tau} = \frac{\partial}{\partial x}\left[f(x)k(\theta)\frac{\partial \theta}{\partial x}\right] - \mathcal{M}^2\theta^{n+1}, \quad 0 < x < 1. \tag{6.15}$$

As proposed by McNabb and Wake [31] we define the mean action time as follows

$$\tau^*_{mean} = \underset{x}{Sup}\int_0^\infty \tau J(x,\tau)d\tau \tag{6.16}$$

where $J(x,\tau)$ is the density function. In our case, the appropriate density function can be established by using a similar approach with regard to the decay process. However, given the presence of a source term we make the additional assumption that $\mathcal{M} << \epsilon$ where $\epsilon$ is some small parameter. This allows us to follow a procedure which requires the equation to be in conserved form. We let $J(x,\tau) = c(x)\dfrac{\partial \theta}{\partial \tau}$ be the density function associated with $\dfrac{\partial \theta}{\partial \tau}$. Then, as per the definition of the density function, we have

$$\int_0^\infty J(x,\tau)d\tau = \int_0^\infty c(x)\frac{\partial \theta}{\partial \tau}d\tau = 1.$$

This means that

$$J(x,\tau) = \frac{\frac{\partial \theta}{\partial \tau}}{\int_0^\infty \frac{\partial \theta}{\partial \tau}d\tau}. \tag{6.17}$$

From equation (6.16) and equation (6.17) we have

$$\tau^*_{mean} = \underset{x}{Sup}\frac{A}{C}$$

$$A = \int_0^\infty \tau \frac{\partial \theta}{\partial \tau} d\tau$$
$$C = \int_0^\infty \frac{\partial \theta}{\partial \tau} d\tau.$$

That is

$$\tau^*_{mean} = \underset{x}{Sup} \frac{\int_0^\infty \tau \frac{\partial \theta}{\partial \tau} d\tau}{\int_0^\infty \frac{\partial \theta}{\partial \tau} d\tau}. \tag{6.18}$$

In our case we don't know details regarding the final steady state. Furthermore, given the non-linearity of the equation and the presence of a source term which makes the equation quite complex, it is difficult to find an associated Green function in order to structure a Poisson equation for the mean action time as proposed by McNabb and Wake [31]. As a consequence, we instead use the results obtained via our relaxation scheme. This approach has been explicitly displayed below.

Let

$$D(x, \tau) = \frac{\partial}{\partial x} \left[ f(x) k(\theta) \frac{\partial \theta}{\partial x} \right] - \mathcal{M}^2 \theta^{n+1}$$

then

$$A(x) = \int_0^\infty \tau D(x, \tau) d\tau \tag{6.19}$$

$$C(x) = \int_0^\infty D(x, \tau) d\tau. \tag{6.20}$$

By employing the finite difference method we have

$$D(x_i, \tau) = \frac{1}{\Delta x_i^2} \left( d(x_{i+1}, x_{i+\frac{1}{2}}, x_i) - d(x_i, x_{i-\frac{1}{2}}, x_{i-1}) \right) - \mathcal{M}^2 \theta^{n+1}(x_i, \tau) + o(\Delta x)^2 \tag{6.21}$$

with

$$d(x_i, x_{i-\frac{1}{2}}, x_{i-1}) = f(x_{i-\frac{1}{2}}) k(\theta(x_{i-\frac{1}{2}}, \tau)) \left( \theta(x_i, \tau) - \theta(x_{i-1}, \tau) \right)$$

where we compute $\theta(x_i, \tau)$ via our numerical relaxation scheme.

Therefore

$$A(x_i) = \lim_{n \to \infty} \sum_{j=1}^{n} \tau_j D(x_i, \tau_j) \Delta \tau_j \tag{6.22}$$

Figure 6.1: *Comparison of the fin efficiency ($\eta$) between a rectangular and exponential profile for $\alpha = 3$, $n = m = 1/4$ with varying $\mathcal{M}$.*

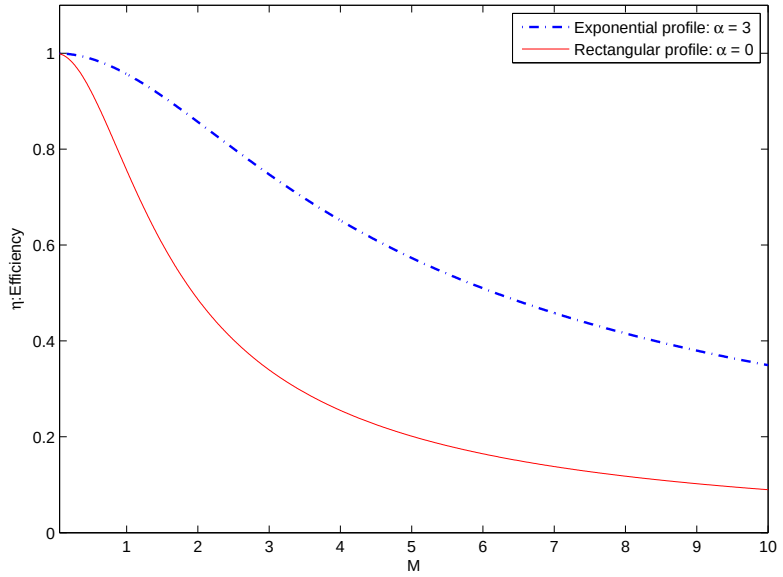


$$C(x_i) = \lim_{n \longrightarrow \infty} \sum_{j=1}^{n} D(x_i, \tau_j) \Delta \tau_j \tag{6.23}$$

and

$$\tau^*(x_i) = \frac{A(x_i)}{C(x_i)}. \tag{6.24}$$

Therefore

$$\tau^*_{mean} = \underset{x_i}{Sup}\{\tau^*(x_i)\}. \tag{6.25}$$

This constitutes our explicit numerical mean action time. The next Section uses these results as a means of measuring the performance of the fin.

## 6.4 Mean action time as a measure of fin performance

One of the most studied and important fin characteristics is the fin efficiency defined as

$$\eta(\mu) = \int_0^1 \theta(x, \mu) dx.$$

Figure 6.1 depicts the fin efficiencies for both a rectangular fin and an exponential fin profile with parameter $\alpha = 3$. As depicted we find that the exponential fin profiles are more efficient than the rectangular fin profiles. This complies with our results which showed that the higher the exponential parameter the more efficient the temperature distribution - see Figures 4.1 and 4.2. The same results have been obtained from steady states solutions by [30] as shown in the graphics provided. Transient solutions are able to provide us with more than just solutions through time however. As shown above these solutions are able to provide us with the transition time between two steady states which plays a major role in the evaluation of the fin performance. Thus far the fin performance is mostly described by the fin tip temperature rise, the fin efficiency and the base heat transfer rate [30] none of which consider the time taken by the temperature distribution process to reach some type of equilibrium.

Even if it is difficult to know exactly how long a process may take to reach an equilibrium, the mean action time is able to provide us with an approximation of the total time taken as suggested by McNabb and Wake [31] and Landman and McGuiness [33]. Therefore, to better analyse the fin performance, we consider the mean action time as a means of obtaining an averaged transition time.

In order to obtain $\tau^*_{mean}$, given how well our relaxation scheme performed against well known benchmark results in Chapter 4, we use the same numerical scheme as a means of computing the mean action time as described in the previous Section. This is done for small values of the thermo-geometric parameter, as per previous discussions, due to the nature of our equation. A computational measure, $\tau_{max}$, of our time taken to equilibrium is obtained by fixing the maximum error between the iterants, i.e. we fix the error allowed as a means of defining computational convergence. This is required, given that in actuality, as per Landman and McGuiness [33], diffusion processes take an infinite amount of time to come to equilibrium. We fix the tip temperature error allowed between the solutions as $\epsilon = 5 \times 10^{-3}$. In order to compare $\tau^*_{mean}$ and $\tau_{max}$ we employ the temperature at the tip; this choice was provided by Turkyilmazoglou [30] where the tip temperature was classified among the most important characteristics of fins studied in engineering heat transfer problems. In many cases, our numerical results took extremely long to converge and as such the time taken to stabilize could not be determined with the hardware available to us. This again is an indication of the difficulties involved in finding the time taken for equilibrium to be reached. Our intention is to propose the mean action time as an additional performance index based on the duration of the process. Tables 6.1, 6.2 and 6.3 show the mean action time for different types of exponential fin profiles. Table 1 is for $\alpha = 0$ (rectangular case), Table 2 for $\alpha = 1$ and Table 3 for $\alpha = 2$. For various values of the thermo-geometric parameter we give the ratio of the solution at the mean action time against the exact solution at the tip, the computed mean action time and the maximum time used for convergence of our numerical solution. We find that the highest times taken to approximately converge to the steady state analytical solutions were extremely high when compared to the mean action times

that were computed. In fact we find that the tip temperature at the mean action time reaches approximately two thirds $(\frac{2}{3})$ of the tip temperature associated with the maximum time taken to convergence. Furthermore, we notice that $\tau_{max}/\tau^*_{mean} \approx 3.7$ (as $\mathcal{M}$ increases this ratio decreases slightly) across the various values of the thermo-geometric parameter which again shows that our methodology produces consistent results especially for small $\mathcal{M}$.

Table 6.1: Mean action time $\tau^*_{mean}$ against $\mathcal{M}$ for $\alpha = 0$ and $n = m = 1/4$

| $\mathcal{M}$ | 0.25 | 0.50 | 0.75 | 1.00 | 1.50 |
|---|---|---|---|---|---|
| $\frac{\theta_{\tau^*_{mean}}(0)}{\theta_{exact}(0)}\%$ | 66.94 | 66.91 | 66.80 | 66.61 | 65.88 |
| $\tau^*_{mean}$ | 0.6016 | 0.5701 | 0.5267 | 0.4797 | 0.3944 |
| $\tau_{max}$ | 2.2784 | 2.1306 | 1.9149 | 1.6677 | 1.2039 |

As such we find that, as per Landman and McGuiness's suggestion [33], we have taken a more averaged approach and determined when the average temperature is a fixed fraction of the final equilibrium value, instead of obtaining the final time taken to reach the steady state. However the fact that this fraction is fixed at two thirds means that this information is useful in determining the time taken for the process to reach equilibrium and hence acts as a means of assessing the performance of the fin in terms of the length of time taken by this process. Furthermore, Tables 6.1, 6.2 and 6.3 show that the mean action time taken to reach a steady state is less for the exponential profiles than for the rectangular case. It is seen that the higher the

values of the exponential parameter $\alpha$, the lower are the corresponding mean action times. This means that for applications that require the process to reach equilibrium fast it would be better to use exponential fin profiles with a larger exponential coefficient parameter. Therefore, one may select an appropriate profile which fulfills the requirement for reaching equilibrium at a certain speed; the only useful performance indicator which can assist in this regard is the mean action time.

Table 6.2: Mean action time $\tau^*_{mean}$ against $\mathcal{M}$ for the exponential profile with $\alpha = 1$ and $n = m = 1/4$

| $\mathcal{M}$ | 0.25 | 0.50 | 0.75 | 1.00 | 1.50 |
|---|---|---|---|---|---|
| $\frac{\theta_{\tau^*_{mean}}(0)}{\theta_{exact}(0)}\%$ | 66.95 | 66.92 | 66.86 | 66.77 | 66.44 |
| $\tau^*_{mean}$ | 0.3217 | 0.3131 | 0.3001 | 0.28447 | 0.2507 |
| $\tau_{max}$ | 1.1856 | 1.1461 | 1.0847 | 1.007 | 0.8292 |

## 6.5 Conclusion

In this Chapter, we have used a numerical approach to compute the mean action time for the process of heat being transferred from the base to the tip of the fin till equilibrium is reached. The novelty of this work is based on the fact that no such numerical study has been conducted previously. Excellent researches have been conducted in [31, 32, 33] on the mean action time of a process but the limitation of these works is that the two steady state temperatures are constant and well known

Table 6.3: Mean action time $\tau^*_{mean}$ against $\mathcal{M}$ for the exponential profile with $\alpha = 2$ and $n = m = 1/4$

| $\mathcal{M}$ | 0.25 | 0.50 | 0.75 | 1.00 | 1.50 |
|---|---|---|---|---|---|
| $\frac{\theta_{\tau^*_{mean}}(0)}{\theta_{exact}(0)}\%$ | 66.90 | 66.88 | 66.82 | 66.76 | 66.52 |
| $\tau^*_{mean}$ | 0.1812 | 0.1786 | 0.1744 | 0.1691 | 0.1563 |
| $\tau_{max}$ | 0.6492 | 0.6353 | 0.6133 | 0.5847 | 0.5155 |

from the beginning of the computation. However this is not the case for several heat transfer problems including our case where the final temperature is not know at start.

Suryanarayana [24, 25] attempted to obtain the equilibrium time, but did so while considering the simplest linear case. He did not manage to obtain the time to steady state exactly even for this linear case. He only computed the time for which the temperature reaches within one percent of its steady state value.

A key contribution of our work is that we managed to numerically compute a mean action time for any physical circumstance without restriction and our results are meaningful as interpreted above. As such we propose the mean action time as a new measure of fin performance. In this manner we are able to contribute to assessment of a fin as an object of heat transfer.

# Chapter 7

# Numerical scheme for a time fractional non-linear heat transfer equation

## 7.1 Introduction

It is important to point out that standard mathematical models of integer order derivatives do not represent all physical cases which are observed among natural phenomena. Several physical phenomena are in part or in full modelled by heat transfer equation with fractional ordered derivatives. Furthermore, these problems are usually modelled by non-linear partial differential equations which often cannot be solved analytically [62] especially for fractional order PDEs. The applications and theory of fractional calculus has been exhaustively investigated and discussed by several researchers [63, 64, 65, 66, 67, 68]. The literature shows that fractional heat transfer can be observed in several situations such as: heat transfer in heterogeneous media [35],

in beam heating [36], in bioheat equation [39], and heat arising in fractal transient conduction [40]. Those are only few situations where the heat transfer modelled via fractional PDE has been considered within a practical context.

In this Chapter, we would like to consider and investigate numerical methods for the solution of nonlinear fractional PDEs. In the literature [35, 36, 37, 38, 39, 69, 70, 71, 72], most problems modelling heat transfer via fractional PDEs, are either linear or quasi-linear and few consider the nonlinear model with a source term; this is then the prime motivation for this work.

In this work, we provide new insights by comparing fractional against integer order numerical schemes to better open doors for further research in this field.

Sierociuk et al. [35] have shown that the differential equation with integer order derivatives describes the heat transfer in solid materials while the heterogeneous media is described either by a sub-diffusion or by hyper-diffusion equations resulting from fractional order PDEs. They have proven that heat transfer in heterogeneous media is better modelled by fractional order PDEs and hence the supremacy of fractional against integer order derivatives to deal with real life problems. Similarly, Dzielinski et al. [36] presented some applications of fractional order calculus and one of the examples considered was the beam heating problem where the fractional order model better represented the physical process. Alkhasov et al. [37] investigated the influence of non-locality of the heat conduction equation in time and space via fractional order derivatives. The findings are that fractional order PDEs permit one to naturally consider the spatial and temporal non-localities in a process of heat transfer. Also,

Kulish and Lage [38] have shown that the transient heat diffusion equation can be transformed into a fractional PDE. Recently, Damor et al. [39] have modelled the heat transfer in biological tissues via fractional order PDEs and they have recorded an elevation in the temperature as the value of the fractional order parameter $\gamma$ decreases; the temperature decreases as the depth of the skin tissue increases.

In most of the literature, it was established that the results for the fractional PDEs matched the corresponding integer-order results. Thus there is no loss of accuracy when one models these problems via fractional order PDEs. Most of the above mentioned literature was limited to considering only linear cases which allowed for the use of transform methods. In addition, most of the real life situations for heterogeneous mediums are more complex and cannot be modelled by linear equation. In this Chapter we will establish a numerical scheme for a one-dimensional time fractional non-linear heat transfer equation and we will compare this against the numerical scheme for the integer order heat transfer equation. Within the scope of fractional calculus, we shall consider a one dimensional heat transfer equation with source term of the form

$$\frac{\partial^\gamma \theta}{\partial \tau^\gamma} = \frac{\partial}{\partial x}\left(f(x)k(\theta)\frac{\partial \theta}{\partial x}\right) - \mathcal{M}^2\theta^{n+1}, \quad 0 < \gamma \leq 1 \tag{7.1}$$

with boundary conditions

$$\frac{\partial \theta}{\partial x}|_{x=0} = 0, \qquad \theta(1,\tau) = 1, \quad \tau > 0$$

$$\theta(x,0) = 0.$$

As such, we are considering a non-linear time fractional partial differential equation. Several approaches have been used to solve fractional partial differential equations [64, **?**, 66]. In some cases, the philosophy of Green function together with some inte-

gral transforms with special functions have played a major role in solving some special problems in fractional calculus [63]. However, the non-linear nature of the problem does not allow us to use the Green's function via either Laplace, Fourier or Mellin transforms and hence take advantage of the convolution theorem.

Therefore, numerical techniques are among the remaining feasible alternatives. On the other hand, numerical techniques can be more complex to implement: finite difference methods require complex discretisations given that numerical differentiation and integration are coupled. For this reason, it is logical to provide fundamental tools of fractional calculus to better provide a logical numerical scheme. The key component shall be a proper discretisation of

$$\frac{\partial^{\gamma}\theta}{\partial\tau^{\gamma}}$$

with the use of a suitable fractional order derivative. As such we need to first establish a suitable derivative for the development of an appropriate numerical scheme.

## 7.2 Fractional order derivative: Background

In fractional calculus we deal with taking real or complex numbers as powers of either the differentiation or integration operators. Therefore, to better build a suitable framework for the remaining part in this Chapter, we introduce basic principles and definitions used in fractional calculus.

### 7.2.1 Successive integration and differentiation operators

Let J stands for an integral operator such that

$$J\{f(x)\} = \int_a^x f(x_1)dx_1$$

that is

$$J^n\{f(x)\} = \int_a^x \int_a^{x_n} \int_a^{x_{n-1}} \qquad \int_a^{x_2} f(x_1)dx_1dx_2 \quad dx_n.$$

Therefore,

$$J^n\{f(x)\} = \frac{1}{(n-1)!}\int_a^x (x-z)^{n-1} f(z)dz \tag{7.2}$$

and this can be established by recurrence via Leibniz's rule of differentiating integrals. Equivalently, equation (7.2)can be written as

$$J^n\{f(x)\} = \frac{1}{\Gamma(n)}\int_a^x (x-z)^{n-1} f(z)dz \tag{7.3}$$

with $\Gamma$ the gamma function defined by

$$\Gamma(x) = \int_0^\infty \tau^{x-1}e^{-\tau}d\tau. \tag{7.4}$$

For $n = \gamma$ real, equation (7.3) becomes

$${}_aJ^\gamma\{f(x)\} = \frac{1}{\Gamma(\gamma)}\int_a^x (x-z)^{\gamma-1} f(z)dz. \tag{7.5}$$

From this expression it is straight forward that

$${}_aJ^{\gamma+\beta}\{f(x)\} = \frac{1}{\Gamma(\gamma+\beta)}\int_a^x (x-z)^{\gamma+\beta-1} f(z)dz \tag{7.6}$$

$${}_aJ^{n-\gamma}\{f(x)\} = \frac{1}{\Gamma(n-\gamma)}\int_a^x (x-z)^{n-\gamma-1} f(z)dz. \tag{7.7}$$

### 7.2.2 Riemann-Liouville fractional order integral

Equation (7.5) constitutes a fundamental expression from which, the Riemann-Liouville fractional integral is defined as

$$ {}_aD_x^{-\gamma}\{f(x)\} = {}_aI_x^{\gamma}\{f(x)\} = \frac{1}{\Gamma(\gamma)} \int_a^x (x-z)^{\gamma-1} f(z) dz. \tag{7.8} $$

Here, $D^-$ stands for the inverse of derivative operator or integral operator. It is from this expression (7.8) that we are able to define the fractional derivative as an inverse of the fractional integral.

### 7.2.3 Riemann-Liouville fractional order derivative

From the definition of the Riemann-Liouville fractional order integral, if we substitute $\gamma$ by $n-\gamma$ with $n-1 < \gamma < n$ we get

$$ {}_aD_x^{-n+\gamma}\{f(x)\} = {}_aI_x^{n-\gamma}\{f(x)\} = \frac{1}{\Gamma(n-\gamma)} \int_a^x (x-z)^{n-\gamma-1} f(z) dz. \tag{7.9} $$

Differentiating the above expression (7.9) $n$ times (by applying the operator $D^n$) we obtain

$$ {}_aD_x^{\gamma}\{f(x)\} = {}_aI_x^{-\gamma}\{f(x)\} = \frac{1}{\Gamma(n-\gamma)} \frac{d^n}{dx^n} \int_a^x (x-z)^{n-\gamma-1} f(z) dz. \tag{7.10} $$

However, the Riemann-Liouville fractional order derivative presents difficulties when dealing with a constant function.

For example, let $f(x) = c$ where $c$ is a constant, then

$$\begin{aligned}
{}_0D_x^{\frac{1}{3}}\{f(x)\} &= \frac{1}{\Gamma(1-\frac{1}{3})}\frac{d}{dx}\left(\int_0^x (x-z)^{(1-\frac{1}{3}-1)}\, c dz\right) \\
&= \frac{c}{\Gamma(\frac{2}{3})}\frac{d}{dx}\left(\int_0^x (x-z)^{-\frac{1}{3}}\, dz\right) \\
&= \frac{c}{\Gamma(\frac{2}{3})}\frac{d}{dx}\left[-\frac{3}{2}(x-z)^{\frac{2}{3}}\right]_0^x \\
&= \frac{c}{\Gamma(\frac{2}{3})}\frac{d}{dx}\left[\frac{3}{2}x^{\frac{2}{3}}\right] \\
&= \frac{c}{\Gamma(\frac{2}{3})}x^{-\frac{1}{3}} \\
&\neq 0.
\end{aligned} \tag{7.11}$$

From this example, it is clear that the Riemann-Liouville fractional order derivative of a constant is not zero. This property disagrees with the variational aspect of derivatives which usually provides information on variation of the functions.

### 7.2.4 Caputo fractional order derivative

One alternative manner of considering fractional order derivatives in a different manner is via the Caputo fractional order derivative defined by

$${}_a^cD_x^\gamma\{f(x)\} = \frac{1}{\Gamma(n-\gamma)}\int_a^x \left((x-z)^{n-\gamma-1}\frac{d^n}{dz^n}f(z)\right)dz, \quad n-1<\gamma<n. \tag{7.12}$$

This time the fractional derivative of a constant is defined as zero as required. However, the Caputo fractional derivative works only for differentiable functions which is

limiting.

There exist a lot of fractional derivative formulae but our aim here is just to introduce tools of fractional calculus that we might need to build our relevant numerical scheme for our fractional non-linear heat transfer equation. In the remaining part of this Chapter, we shall use the fractional derivative in the sense of Caputo represented by equation (7.12).

## 7.3 Numerical scheme

In this Section we consider the non-linear one dimensional time fractional heat equation of the form

$$\frac{\partial^\gamma \theta}{\partial \tau^\gamma} = \frac{\partial}{\partial x}\left(f(x)k(\theta)\frac{\partial \theta}{\partial x}\right) - \mathcal{M}^2\theta^{n+1}, \quad 0 < \gamma \leq 1 \tag{7.13}$$

under initial and boundary conditions as provided by (7.1). Let the value of $\theta(x,\tau)$ at grid point $(x_i,\tau_j)$ be denoted by $\theta_i^j = \theta(x_i,\tau_j)$. Let us first provide a discrete approximation of the Caputo fractional derivative $\dfrac{\partial^\gamma \theta}{\partial \tau^\gamma}$ at $(x_i,\tau_{j+\frac{1}{2}})$. In fact, by the definition of the Caputo fractional order derivative we have

$$\frac{\partial^\gamma \theta}{\partial \tau^\gamma}(x_i,\tau_{j+\frac{1}{2}}) = \frac{1}{\Gamma(1-\gamma)}\int_0^{\tau_{j+\frac{1}{2}}}\left((\tau_{j+\frac{1}{2}}-z)^{-\gamma}\frac{d\theta_i(z)}{dz}\right)dz. \tag{7.14}$$

The right hand side of equation (7.14) is a definite integral which shall be approximated via Riemann sums. Let

$$I = \int_0^{\tau_{j+\frac{1}{2}}}\left((\tau_{j+\frac{1}{2}}-z)^{-\gamma}\frac{d\theta_i(z)}{dz}\right)dz. \tag{7.15}$$

By linearity of the definite integral we have

$$I = I_1 + I_2 \tag{7.16}$$

with

$$I_1 = \int_0^{\tau_j} \left( (\tau_{j+\frac{1}{2}} - z)^{-\gamma} \frac{d\theta_i(z)}{dz} \right) dz$$

and

$$I_2 = \int_{\tau_j}^{\tau_{j+\frac{1}{2}}} \left( (\tau_{j+\frac{1}{2}} - z)^{-\gamma} \frac{d\theta_i(z)}{dz} \right) dz.$$

At $\tau_{j+\frac{1}{2}}$ we have

$$\frac{\partial \theta_i(\tau_{j+\frac{1}{2}})}{\partial \tau} = \frac{\theta_i(\tau_{j+1}) - \theta_i(\tau_j)}{\Delta\tau} + o(\Delta\tau) \tag{7.17}$$

as per a forward finite difference approximation. Therefore

$$\begin{aligned}
I_2 &= \frac{\theta_i(\tau_{j+1}) - \theta_i(\tau_j)}{\Delta\tau} \int_{\tau_j}^{\tau_{j+\frac{1}{2}}} \left( (\tau_{j+\frac{1}{2}} - z)^{-\gamma} dz \right) dz + o(\Delta\tau) \\
&= \frac{\theta_i^{j+1} - \theta_i^j}{\Delta\tau} \frac{-1}{1-\gamma} \left[ (\tau_{j+\frac{1}{2}} - z)^{1-\gamma} \right]_{j\Delta\tau}^{(j+1/2)\Delta\tau} + o(\Delta\tau) \\
&= \frac{\theta_i^{j+1} - \theta_i^j}{\Delta\tau} \frac{1}{1-\gamma} \left[ ((j+1/2)\Delta\tau - j\Delta\tau)^{1-\gamma} \right] + o(\Delta\tau) \\
&= \frac{\theta_i^{j+1} - \theta_i^j}{\Delta\tau} \frac{1}{1-\gamma} \left( \frac{1}{2}\Delta\tau \right)^{1-\gamma} + o(\Delta\tau).
\end{aligned} \tag{7.18}$$

It means that

$$I_2 = \frac{\theta_i^{j+1} - \theta_i^j}{\Delta\tau} \frac{1}{1-\gamma} \frac{1}{2^{1-\gamma}} (\Delta\tau)^{1-\gamma} + o(\Delta\tau). \tag{7.19}$$

If we subdivide the intervals $[\tau_{k-1}, \tau_k], \quad k = 1, 2, 3, ..., j$ of $[0, \tau_j]$, then

$$\begin{aligned} I_1 &= \int_0^{\tau_j} \left( (\tau_{j+\frac{1}{2}} - z)^{-\gamma} \frac{d\theta_i(z)}{dz} \right) dz \\ &= \sum_{k=1}^{j} \int_{(k-1)\Delta\tau}^{k\Delta\tau} \left( ((j+1/2)\Delta\tau - z)^{-\gamma} \frac{d\theta_i(z)}{dz} \right) dz \\ &= \sum_{k=1}^{j} \frac{\theta_i^k - \theta_i^{k-1}}{\Delta\tau} \int_{(k-1)\Delta\tau}^{k\Delta\tau} ((j+1/2)\Delta\tau - z)^{-\gamma} \, dz + o(\Delta\tau) \\ &= \sum_{k=1}^{j} \frac{\theta_i^k - \theta_i^{k-1}}{\Delta\tau} \frac{-1}{1-\gamma} \left[ ((j+1/2)\Delta\tau - z)^{1-\gamma} \right]_{(k-1)\Delta\tau}^{k\Delta\tau} + o(\Delta\tau). \end{aligned} \tag{7.20}$$

Therefore

$$I_1 = \frac{\Delta\tau^{(1-\gamma)}}{1-\gamma} \sum_{k=1}^{j} \frac{\theta_i^k - \theta_i^{k-1}}{\Delta\tau} \left[ \left( (j-k+\frac{3}{2}) \right)^{1-\gamma} - \left( (j-k+\frac{1}{2}) \right)^{1-\gamma} \right] + o(\Delta\tau). \tag{7.21}$$

Substituting equations (7.19) and (7.21) into (7.16) gives

$$\begin{aligned} I &= \frac{\Delta\tau^{(1-\gamma)}}{1-\gamma} \sum_{k=1}^{j} \frac{\theta_i^k - \theta_i^{k-1}}{\Delta\tau} \left[ \left( (j-k+\frac{3}{2}) \right)^{1-\gamma} - \left( (j-k+\frac{1}{2}) \right)^{1-\gamma} \right] \\ &+ \frac{1}{2^{1-\gamma}} \frac{\Delta\tau^{(1-\gamma)}}{1-\gamma} \frac{\theta_i^{j+1} - \theta_i^j}{\Delta\tau} + o(\Delta\tau). \end{aligned} \tag{7.22}$$

From (7.14), (7.15) and (7.22), we get at $(\tau_{j+\frac{1}{2}})$

$$\begin{aligned} \frac{\partial^\gamma \theta_i}{\partial \tau^\gamma} &= \frac{\Delta\tau^{(1-\gamma)}}{\Gamma(2-\gamma)} \sum_{k=1}^{j} \frac{\theta_i^k - \theta_i^{k-1}}{\Delta\tau} \left[ \left( (j-k+\frac{3}{2}) \right)^{1-\gamma} - \left( (j-k+\frac{1}{2}) \right)^{1-\gamma} \right] \\ &+ \frac{1}{2^{1-\gamma}} \frac{\Delta\tau^{(1-\gamma)}}{\Gamma(2-\gamma)} \frac{\theta_i^{j+1} - \theta_i^j}{\Delta\tau} + o(\Delta\tau). \end{aligned} \tag{7.23}$$

Equation (7.23) represents the discrete approximation of the left hand side of the fractional partial differential equation (7.13).

As it has been exhaustively motivated in Chapter 4, the relaxation numerical schemes are simple to implement and are able to achieve higher order accuracy in capturing weak solutions without using Riemann solvers [27, 52, 53]. Following all steps as established in Chapter 4, the zero relaxation numerical scheme for the fractional heat transfer equation under discussion is

$$\frac{\partial^\gamma \theta}{\partial \tau^\gamma} = -\frac{1}{2\Delta x_i}\left(F_{i+1} - F_{i-1}\right) + \frac{a}{2\Delta x_i}\left(\theta_{i+1} - 2\theta_i + \theta_{i-1}\right) - \mathcal{M}^2\theta_i^{n+1} \tag{7.24}$$

with

$$F_i = f(x_i)k(\theta_i)\frac{\theta_{i+1} - \theta_{i-1}}{2\Delta x_i}.$$

From equation (7.13), matching its left hand side provided by (7.23) with its right hand side (7.24) we obtain

$$\frac{\Delta\tau^{(1-\gamma)}}{\Gamma(2-\gamma)}\sum_{k=1}^{j}\frac{\theta_i^k - \theta_i^{k-1}}{\Delta\tau}\left[\left((j-k+\frac{3}{2})\right)^{1-\gamma} - \left((j-k+\frac{1}{2})\right)^{1-\gamma}\right] + \frac{1}{2^{1-\gamma}}\frac{\Delta\tau^{(1-\gamma)}}{\Gamma(2-\gamma)}\frac{\theta_i^{j+1} - \theta_i^j}{\Delta\tau}$$

$$= -\frac{1}{2\Delta x_i}\left(F_{i+1} - F_{i-1}\right) + \frac{a}{2\Delta x_i}\left(\theta_{i+1}^j - 2\theta_i^j + \theta_{i-1}^j\right) - \mathcal{M}^2(\theta_i^j)^{n+1}. \tag{7.25}$$

Therefore,

$$\theta_i^{j+1} = \theta_i^j + 2^{1-\gamma}\sum_{k=1}^{j}\left[\left((j-k+\frac{3}{2})\right)^{1-\gamma} - \left((j-k+\frac{1}{2})\right)^{1-\gamma}\right]\left(\theta_i^k - \theta_i^{k-1}\right)$$

$$+2^{1-\gamma}\Gamma(2-\gamma)\Delta\tau^\gamma\left[-\frac{1}{2\Delta x_i}\left(F_{i+1} - F_{i-1}\right) + \frac{a}{2\Delta x_i}\left(\theta_{i+1}^j - 2\theta_i^j + \theta_{i-1}^j\right) - \mathcal{M}^2(\theta_i^j)^{n+1}\right]. \tag{7.26}$$

Equation (7.26) represents an explicit numerical scheme of our one dimensional time fractional non-linear heat equation with source term.

## 7.4 Numerical results

### 7.4.1 Model validation

It is very important to point out that no results in the literature have been found as benchmark results to use for our computational solutions obtained in this Section.

It is important to validate our numerical results so that we may confirm the relevance of our scheme; inaccurate physical results need to be avoided. The non-linear nature and presence of a source term may make it impossible to study analytically the stability and convergence of our numerical scheme. Therefore, we would like to validate the approach before implementation.

For this reason, we are going to test our fractional numerical scheme by considering the case when $\gamma = 1$. This will allow us to either validate the model or question it since we have a number of benchmark results to compare with.
For practical purposes we consider the heat transfer in a one dimensional exponential fin profile. In this case,

$$f(x) = e^{\alpha x}$$

and

$$k(\theta) = \theta^m.$$

Figure 7.1: *Temperature distribution for exponential fin profiles for* $\mathcal{M} = 2.5$, $\alpha = 1$ *(top) and* $\alpha = 2$ *(bottom) with* $n = m = 0,\ 1/3,\ 2$ *and* $3$ *obtained via the numerical scheme (____) compared to a steady state solution (∘ ∘ ∘∘).*

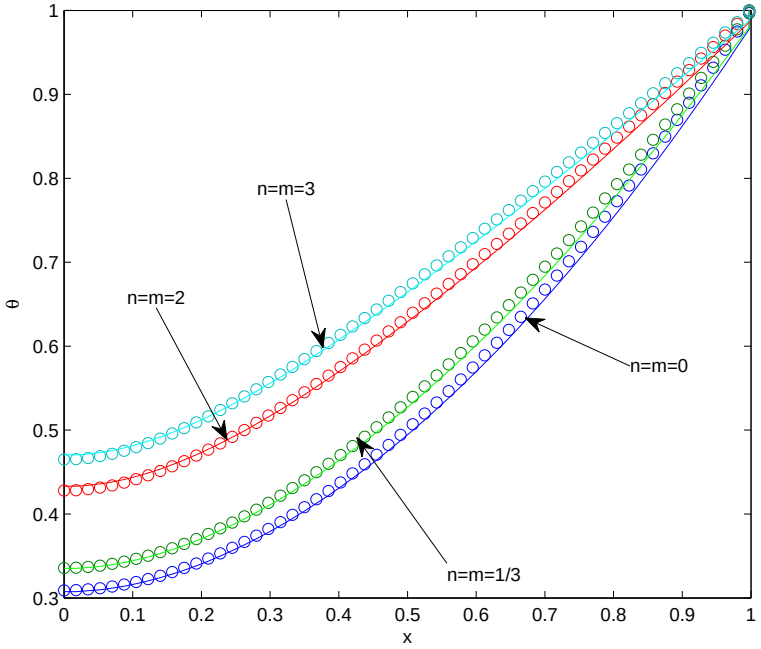


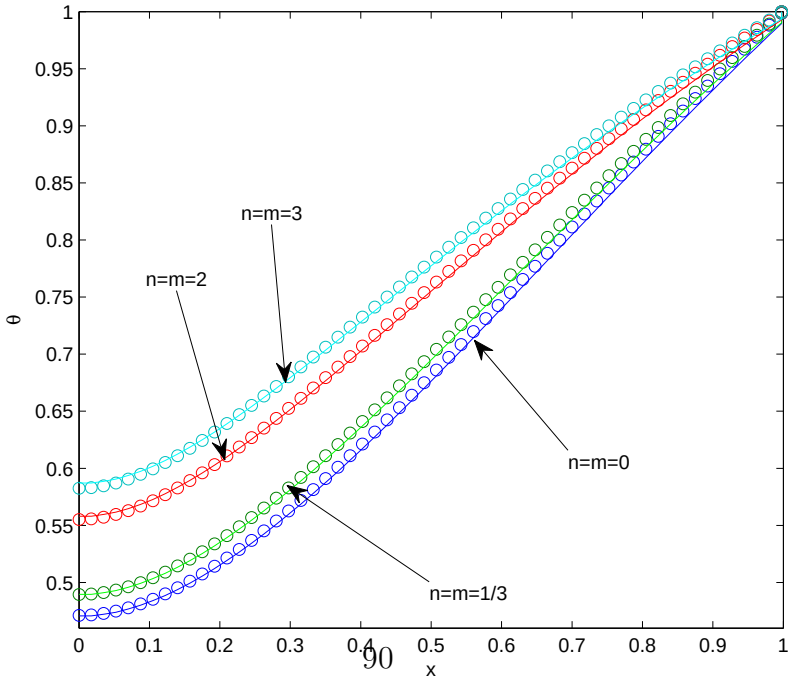

Figure 7.2: *Temperature distribution for exponential fin profiles for* $\mathcal{M} = 2.5$, $\alpha = 3$ *(top) and* $\alpha = 4$ *(bottom) with* $n = m = 0,\ 1/3,\ 2$ *and* $3$ *obtained via the numerical scheme (____) compared to a steady state solution (∘ ∘ ∘∘).*

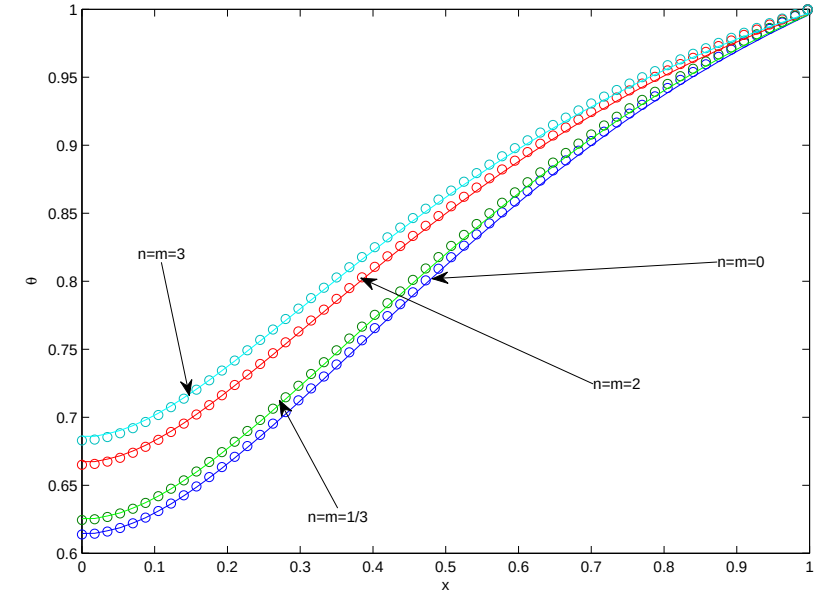


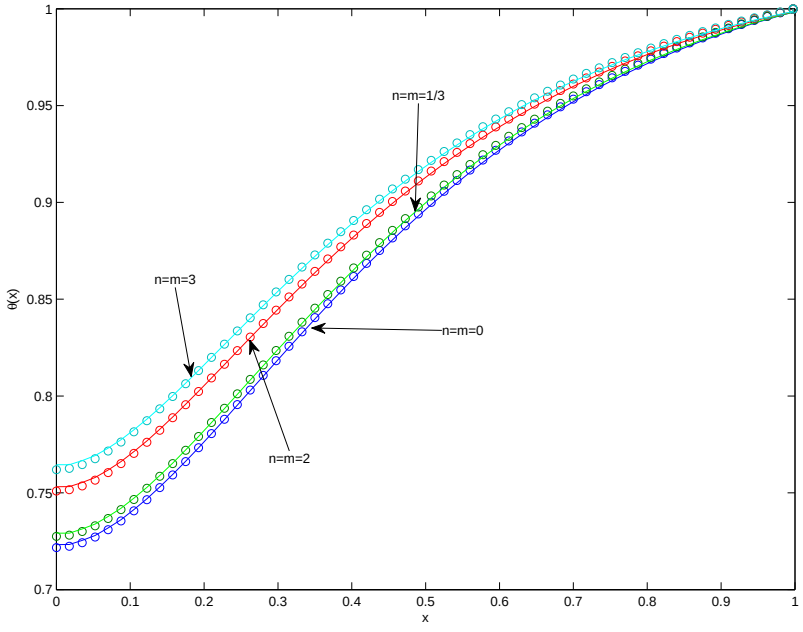

Figure 7.3: *Temperature distribution for different values of* $\gamma$ *and* $\mathcal{M} = 0.01$.

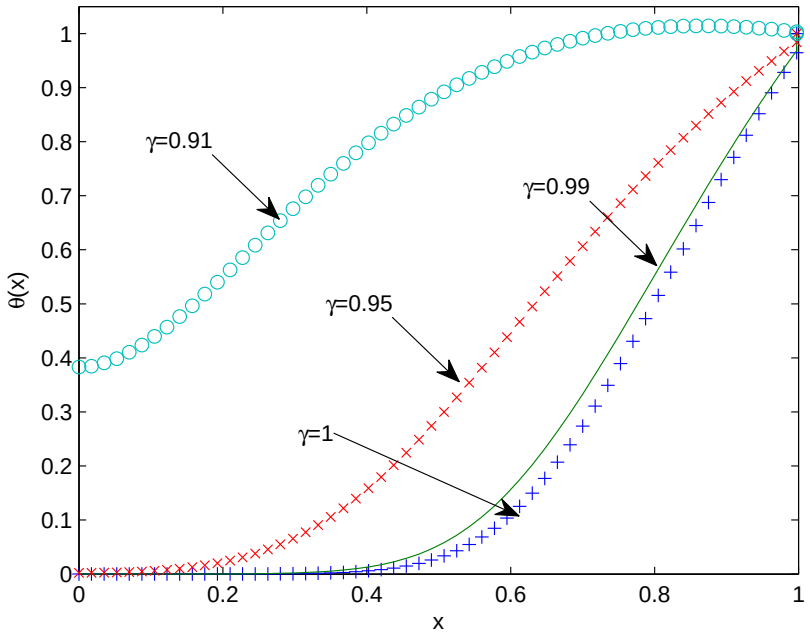


Figure 7.4: *Temperature distribution for* $\gamma = 0.91$ *and different values of* $M$.

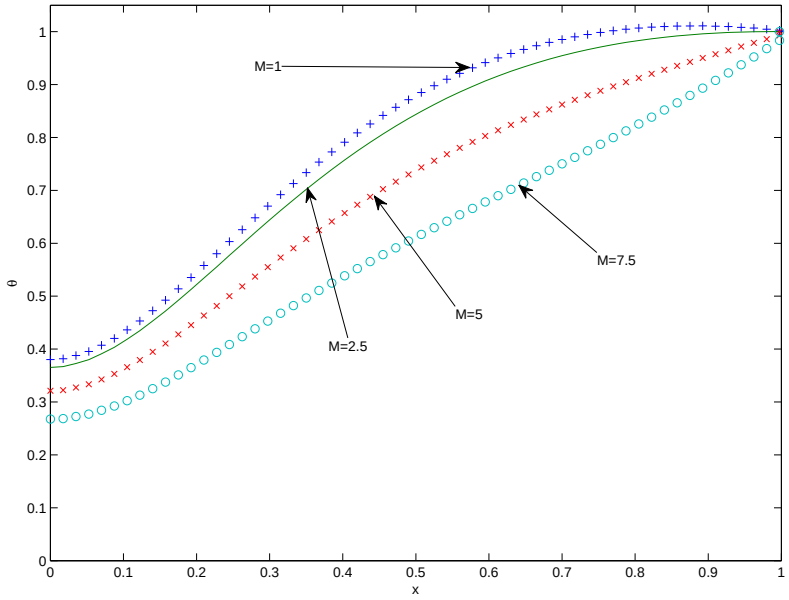

Figure 7.5: *Temperature distribution for* $\gamma = 0.95$ *and different values of* $M$*.*

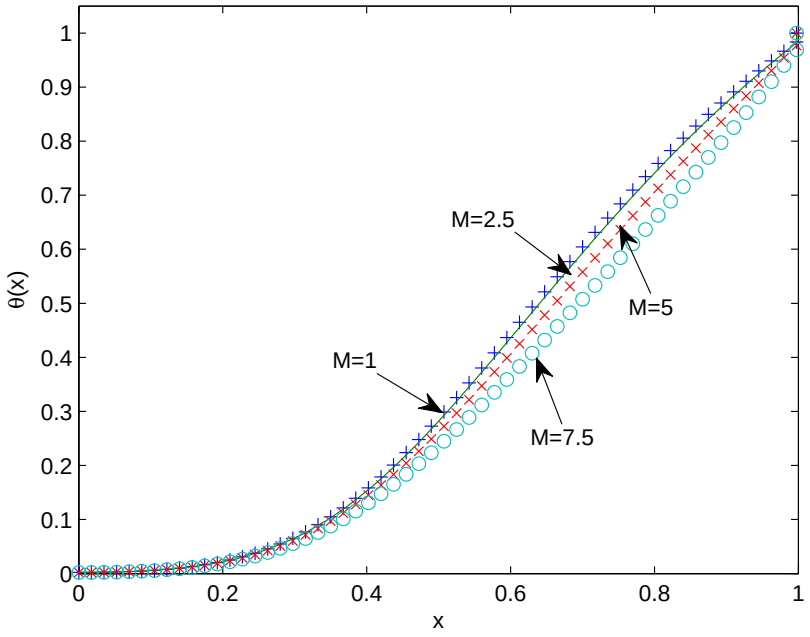


That is

$$\frac{\partial^\gamma \theta}{\partial \tau^\gamma} - \frac{\partial}{\partial x}\left(e^{\alpha x}\theta^m \frac{\partial \theta}{\partial x}\right) = -\mathcal{M}^2\theta^{n+1}. \tag{7.27}$$

This problem has steady state exact solutions and we will compare these exact solutions against the numerical solutions obtained via our numerical scheme for $\tau \to \infty$. We will do so for four different cases.

**Case 1: n=m=0**

In this case we have a constant heat flow [30]

$$\frac{\partial^\gamma \theta}{\partial \tau^\gamma} - \frac{\partial^2 \theta}{\partial x^2} = -\mathcal{M}^2\theta. \tag{7.28}$$

This is the case considered mostly by different researchers often without the source term as well. Figures 7.1 and 7.2 indicate that the results differ significantly for

different values of $n$ and $m$. In each Figure we find that the four curves are clearly different highlight the fact that any simplification rendering $n = m = 0$ will change the problem dramatically.

**Case 2: n=m=1/3**

$$\frac{\partial^\gamma \theta}{\partial \tau^\gamma} - \frac{\partial}{\partial x}\left(e^{\alpha x}\theta^{1/3}\frac{\partial \theta}{\partial x}\right) = -\mathcal{M}^2\theta^{4/3}. \tag{7.29}$$

This case has been referred to as turbulent natural convection and considered in [30].

**Case 3: n=m=2**

$$\frac{\partial^\gamma \theta}{\partial \tau^\gamma} - \frac{\partial}{\partial x}\left(e^{\alpha x}\theta^{2}\frac{\partial \theta}{\partial x}\right) = -\mathcal{M}^2\theta^{4}. \tag{7.30}$$

This case has been referred to as nucleate boiling and discussed in [30].

**Case 4: n=m=3**

$$\frac{\partial^\gamma \theta}{\partial \tau^\gamma} - \frac{\partial}{\partial x}\left(e^{\alpha x}\theta^{3}\frac{\partial \theta}{\partial x}\right) = -\mathcal{M}^2\theta^{4}. \tag{7.31}$$

This case has been referred to as radiation [30]. In cases 2-4 one finds that these equations cannot easily be handled analytically. In Figures 7.1 and 7.2, for different values of the exponential coefficient $\alpha$, we showed the different curves for $m = n = 0$, $m = n = 1/3$, $m = n = 2$ and $m = n = 3$ in each figure to point out the effect when one simplifies the problem into trivial cases. We have varied the exponential parameters from $\alpha = 1$ till $\alpha = 4$ and it is always clear that the solutions differ from the linear to the non-linear case.

Figure 7.6: *Temperature distribution for* $\gamma = 1$, $\mathcal{M} = 0.01$ *and varying time* $\tau$.

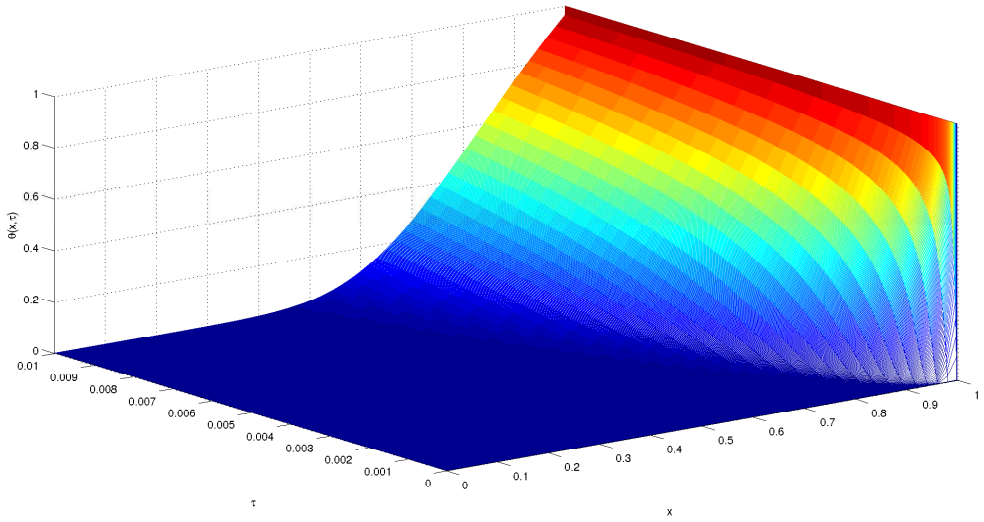


### 7.4.2 Results for $0 < \gamma < 1$

It is seen that for $\gamma = 1$ the scheme (7.26) reduces to the scheme (4.36). In this Section, we analyse different values of the fractional-order parameter $\gamma$ and various values of the thermo-geometric fin parameter $\mathcal{M}$. We consider two-and three-dimensional profiles for this analysis. Fig. 7.3 indicates that a decrease of $\gamma$ implies a dramatic increase of the temperature and the temperature decreases as the length of the fin increases. This complies exactly with the findings of Damor et al. [39]. Furthermore, for varying values of the thermo-geometric parameter $\mathcal{M}$, $\gamma = 0.91$ and $\gamma = 0.95$, the temperature profile decreases with the increase of $\mathcal{M}$ as presented in Fig. 7.4 and Fig. 7.5. The scheme reproduces similar behaviour such as classical solutions where the temperature distribution is a decreasing function of $\mathcal{M}$ [26].

For better visualization we consider a three-dimensional representation which shows how the temperature is distributed spatially across time. Fig.7.6 shows the surface

Figure 7.7: *Temperature distribution for* $\gamma = 0.99$, $\mathcal{M} = 0.01$ *and varying time* $\tau$.

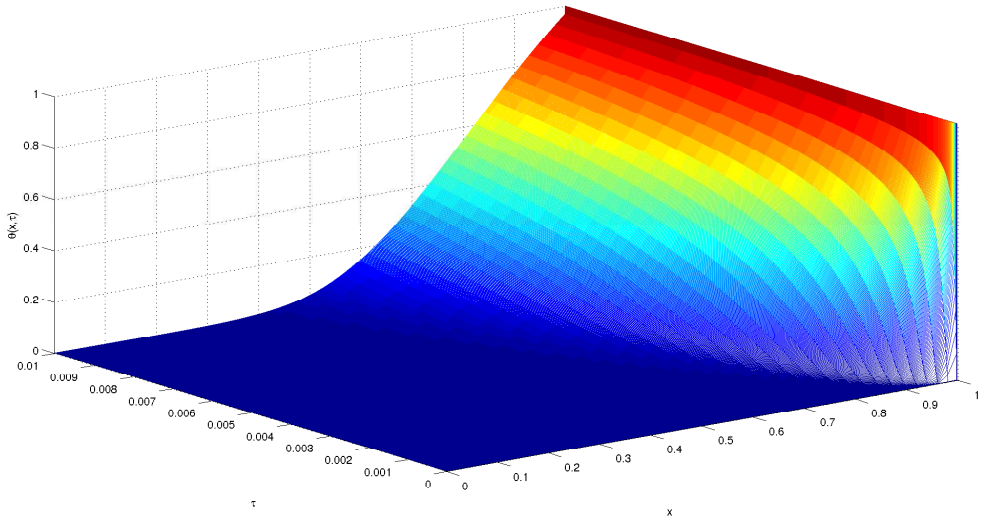


Figure 7.8: *Temperature distribution for* $\gamma = 0.95$, $\mathcal{M} = 0.01$ *and varying time* $\tau$.

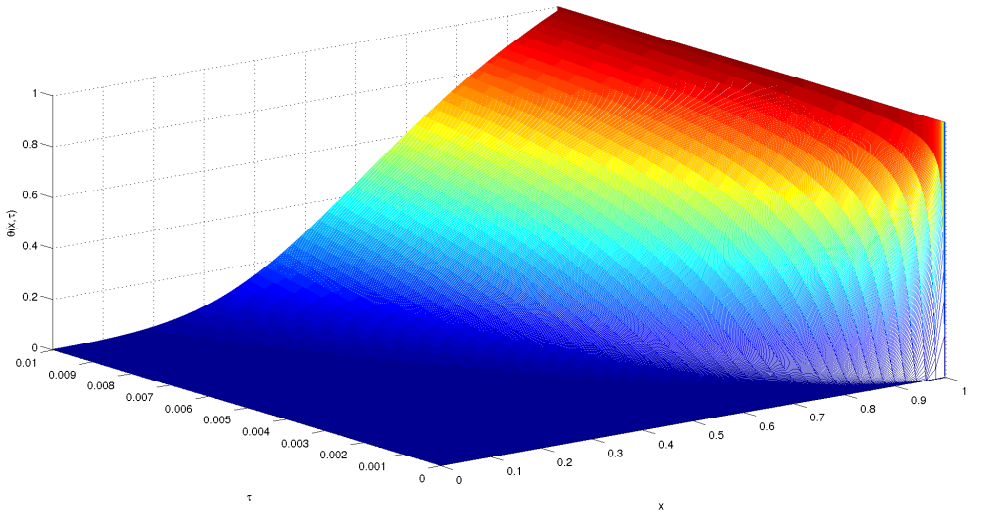

Figure 7.9: *Temperature distribution for* $\gamma = 0.91$, $\mathcal{M} = 0.01$ *and varying time* $\tau$.

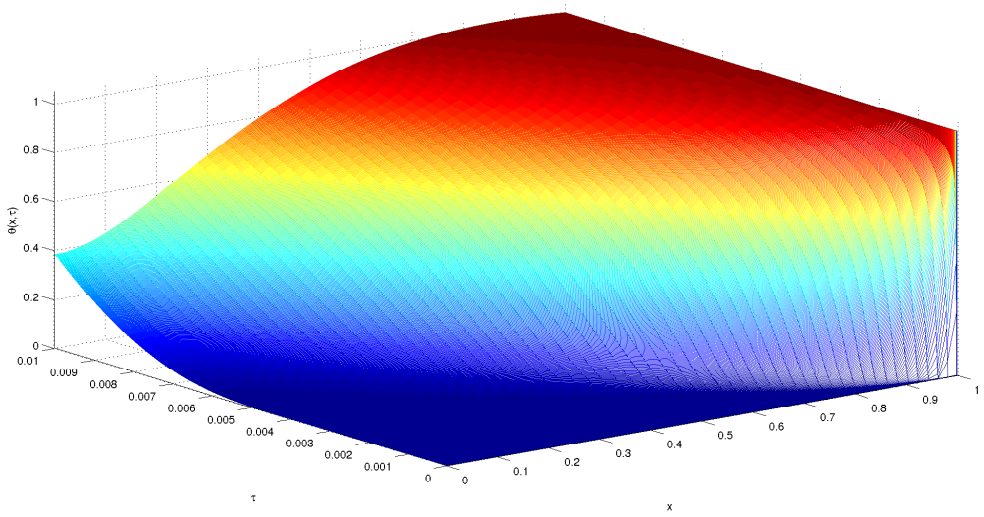


plot of the temperature distribution for $\gamma = 1$, Fig. 7.7 is for $\gamma = 0.99$, Fig. 7.8 is for $\gamma = 0.95$, and Fig. 7.9 is for $\gamma = 0.91$. These figures show that the temperature profile is a decreasing function of $\gamma$ and an increasing function of time $\tau$ and this complies with results in literature [1, 26, 39].

## 7.5 Conclusion

Equation (7.26) is an explicit numerical scheme established from a one dimensional time fractional non-linear heat transfer equation with source term (7.1). This scheme was obtained via a relaxation approach coupled with the discrete approximation for the Caputo fractional derivative of $\dfrac{\partial^\gamma \theta}{\partial \tau^\gamma}$. The novelty of our numerical scheme comes from the above combination of techniques attempted for the first time to the best of our knowledge.

It is very important to point out that for $\gamma = 1$ our fractional numerical scheme verifies the benchmark results obtained by classical schemes. Further, it also matches solutions obtained in earlier Chapters.

One important outcome is that our fractional scheme is more general given that it is able to reproduce results for $0 < \gamma \leq 1$. For $0 < \gamma < 1$ results behave similar to classical results and this confirms that our numerical scheme is able to provide physically meaningful results. Establishing an effective numerical scheme for a fractional heat transfer equation is an important contribution given the wide range of physical applications such as modelling heat transfer in heterogeneous media, beam heating, and bioheat [35, 36, 39] of this model.

# Chapter 8

# Conclusion

The solution of equations modelling heat transfer in one dimensional longitudinal fins has been investigated in this thesis. Due to the limitation of analytical methods, different numerical schemes have been established. The complexity of the problem is increased due to the non-linear nature of the PDE and the presence of a non-linear source term. In the literature some singular geometries were approximated by simpler geometries as a means of guaranteeing analytical solutions [11]. Similarly, some numerical attempts encountered problems for those singular geometries as adiabatic conditions were not fulfilled [1].

In order to obtain solutions to the problem at hand, we developed numerical schemes such as the well-balancing and relaxation numerical schemes. Each numerical scheme contributes new insights while the assumptions made are physically appropriate and meaningful. Moreover, in all of our computations we have maintained the original geometries of our problem. The numerical schemes established have improved upon the results in literature [1, 11]. Furthermore, we have extended our problem to its

variant with fractional order derivatives and the corresponding fractional numerical scheme reproduces consistent results when the fractional order parameter is one.

## 8.1 Limitations of analytical methods

It is already known that analytical solutions are most sought after given their accuracy and usefulness in validating numerical results; unfortunately obtaining these solutions is not always possible. In the literature it is found that the problem is often simplified in order to implement analytical methods [11]. We choose to deal with the original non-linear problem instead of the simplified expression just for the sake of obtaining an analytical solution. Therefore, we turned to numerical methods which allow us to solve the problem as it stands. For this purpose we have successfully constructed powerful numerical schemes that may be used even for cases with singularities for which some techniques have failed in the past [1].

## 8.2 Numerical analysis

From the literature, see [1], some numerical approaches provided unreasonable results for singular fin-types such as the triangular profile. In our research, we managed to establish a scheme which requires no additional assumptions and is capable of dealing with physical singularities in the problem. We have constructed a numerical well-balanced scheme as well as a relaxation numerical scheme both of which obtain efficient and highly accurate solutions [26, 62]. The key contribution of this thesis is the incorporation of the zero-flux boundary condition and the source balancing law obtained from the steady state condition for the well-balanced scheme. Furthermore, the constructed numerical schemes reduce the order of differentiation of the heat

transfer equation to a first order non-linear hyperbolic system of equations. This reduction of order simplifies the problem without omitting any component of the original problem. The results have been validated in Rusagara and Harley [62] where we established a numerical mean action time scheme and proposed it as a measure of fin performance.

Finally, as the integer order PDEs cannot describe heat transfer in heterogeneous media we decided to establish a numerical scheme appropriate to fractional PDEs which can describe heat transfer in heterogeneous media according to Sierociuk et al. [35]. The same established scheme can handle models for beam heating and it has been shown by Dzielinski et al. [36] that the fractional order model allows one to better represent the physical process. The numerical scheme established in this thesis was tested for the case $\gamma = 1$ which confirmed the behaviour of the results obtained. Figures 7.1 and 7.2 show that our fractional numerical scheme for $\gamma = 1$ matches benchmark results obtained via more classical schemes. This work contributes a generalized numerical scheme which provide solutions to problems with many applications [39, 63, 69].

## 8.3 Concluding remarks

The aim of this thesis was to provide effective numerical schemes appropriate for the solution of a non-linear partial differential equation modelling the heat transfer in a one dimensional longitudinal fin. We established three novel numerical approaches to our problem namely the well-balanced, and relaxation scheme as well as an explicit scheme for the fractional version of the heat transfer equation.

All of our numerical schemes verify the benchmark results discussed. As such, we were able to use one of them to construct a numerical expression for the mean action time which was proposed as a measure of fin performance for the first time. This measure has not previously been proposed by researchers as a measure of fin performance because it is difficult to compute in most cases. Further expansions to the research conducted would be to consider higher dimensions. Given the methods employed however this can easily be done.

# Bibliography


[1] R. J. Moitsheki and C. Harley; *Transient heat transfer in longitudinal fins of various profiles with temperature-dependent thermal conductivity and heat transfer coefficient*; Pramana Journal of Physics 77 (2011) 519-532.

[2] V. D. Rao, S.V. Naidu, B. G. Rao, K.V. Sharma; *Heat transfer from a horizontal fin array by natural convection and radiation - a conjugate analysis*; International Journal of Heat and Mass Transfer 49 (2006) 3379-3391.

[3] E.M. Sparrow, S.B. Vemuri; *Natural convection-radiation heat transfer from highly populated pin-fin arrays*; Journal of Heat Transfer 107 (1985) 190-197.

[4] S. Kiwana and M.A. Al-Nimr; *Using porous fins for heat transfer enhancement*; Journal of Heat Transfer 123 (2001) 790-795.

[5] S. Y. Kim, J. W. Paek, and B. H. Kand; *Flow and heat transfer correlations for porous fin in a plate-fin heat exchanger*; Journal of Heat Transfer 122 (2000) 572-578.

[6] Y.J. Lee, P.S. Lee, and S.K. Chou; *Enhanced thermal transport in microchannel using obliques fins*; Journal of Heat Transfer 134 (2012) doi:10.1115/1.4006843.

[7] Y.J. Lee, P.S. Lee, and S.K. Chou; *Numerical study of fluid flow and heat transfer in the enhanced microchannel using obliques fins*; Journal of Heat Transfer 135 (2013) doi:10.1115/1.4023029.

[8] R. Hassanzadeh and H. Pekel; *Heat transfer enhancement in annular fins functionally graded materials*; Heat Transfer- Asian Research 42(7)(2013) 603-617.

[9] J.Y. Jang, L.F. Hsu, and J.S. Leu; *Optimization of the span angle and location of vortex generators in plate-fin and tube exchanger*; International Journal of Heat and Mass Transfer 67(2013) 432-444.

[10] Y.B. Tao, Y.L. He, J. Huang, Z.G. Wu, and W.Q. Tao; *Numerical study of local transfer heat coefficient and fin efficiency of wavy fin-and-tube heat exchangers*; International Journal of Thermal Sciences 46(2007) 768-778.

[11] A. D. Kraus, A. Aziz, J. Welty; *Extended surface heat transfer*; A Wiley-Interscience Publication (2001).

[12] A. Guvenc, H. Yancu; *An experiment investigation on performance of fins on a horizontal base in a free convection heat transfer*; Heat Mass Transfer 37 (2001) 409-416.

[13] A. I. Zografos, J. E. Sunderland; *Natural Convection from pin fin arrays*; Experimental Thermal and Fluid Science 3 (1990) 440-449.

[14] E.M. Sparrow, S.B. Vemuri; *Orientation effects on natural convection or radiation pin-fin arrays*; International Journal of Heat and Mass Transfer. 29(1986)359-368.

[15] G. Guglielmini, E. Nannel, G. Tanda; *Natural convection and radiation heat transfer from staggered vertical fins*; IInternational Journal of Heat and Mass Transfer 30 (1987)1941-1948.

[16] H. Yuncu, G. Anbar; *An experimental investigation on performance of fins on a horizontal base in free convection heat transfer*; Heat and Mass Transfer 33 (1998) 507-514.

[17] R. Rao, S.P. Venkateshan; *Experimental study of free convection and radiation in horizontal fin arrays*; International Journal of Heat and Mass Transfer 39 (1996) 779-789.

[18] W. Wang, C.W. Shu, H.C. Yee and B. Sjogreen; *On well-balanced schemes for non-equilibrium flow with stiff source terms*; Center for Turbulence Research, Annual Research Briefs (2008)391-402.

[19] S. Noelle, N. Pankratz, G. Puppo, and J.R. Natvig; *Well-balancing finite volume schemes of arbitrary order of accuracy for shallow water flows.*; Journal of Computational Physics 213(2006) 474-499.

[20] W. Wang, H.C. Yee, B.Sjongree, T. Margin and C.W. Shu; *Construction of low-dissipative high-order well-balanced filter schemes for non-equilibrium flows*; Center for Turbulence Research, Annual Research Briefs (2009)409-421.

[21] R.J Leveque; *Balancing source terms and flux gradients in higher-resolution Godunov methods: the quasi-steady wave propagation algorithm*; Journal of Computational Physics 146(1998)346-365.

[22] D. Amadori, L. Gosse and G. Guerra; *Global BV entropy solutions and uniqueness for hyperbolic systems of balance laws*; Archive for Rational Mechanics and Analysis 162 (2002) 327-366.

[23] L. Gosse, G. Toscani; *Transient radiative transfer in the grey case: Well-balanced and asymptotic preserving schemes built on case's elementary solutions*; Journal of Quantitative Spectroscopy and Radiative Transfer 112(2011)1995-2012.

[24] N. V. Suryanarayana; *Transient response of straight fins*; ASME Journal of Heat Transfer 97 (1975) 417-423.

[25] N. V. Suryanarayana; *Transient response of straight fins*; ASME Journal of Heat Transfer 98 (1976) 324-326.

[26] I. Rusagara, C. Harley; *A numerical well-balanced scheme for one dimensional heat transfer in longitudinal triangular fins*; Mathematical Problems in Engineering (2013), doi:10.1155/2013/609536.

[27] S. Jin and Z. Xin; *The relaxation schemes for systems of conservation laws in arbitrary space dimensions*; Communications on Pure and Applied Mathematics 48 (1995) 235-276.

[28] R. Kumar and M.K. Kadalbajoo; *Efficient high-resolution relaxation schemes for hyperbolic systems of conservation laws*; International Journal for Numerical Methods in Fluids 55(2007) 483-507.

[29] G. Naldi, L. Pareschi and G.Toscani; *Relaxation schemes for partial differential equations and applications to degenerate diffusion problems*; Survey on mathematics for industry 10:4(2002)315-343

[30] M. Turkyilmazoglu; *Exact solutions to heat transfer in straight fins of varying exponential shape having temperature dependent properties*; International Journal of Thermal Sciences 55 (2012) 69-79.

[31] A. McNabb and G. C. Wake; *Heat conduction and finite measures for transition between steady states*; IMA Journal of Applied Mathematics 47 (1991) 193-206.

[32] A. McNabb; *Means action times, time lags, and mean first passage times for some diffusion problems*; Mathematical and Computer Modelling 18(10) (1993) 123-129.

[33] K. Landman and M. McGuiness; *Mean action time for diffusive process*; Journal of Applied Mathematics and Decision Sciences 4(2) (2000) 125-141.

[34] F. Khani and A. Aziz; *Thermal analysis of a longitudinal trapezoidal fin with temperature-dependent thermal conductivity and heat transfer coefficient*; Communications in Nonlinear Science and Numerical Simulation 15 (2010) 590-601.

[35] D. Sierociuk, A. Dzielinski, G. Sarwas, I. Petras, I. Podlubny, and T. Skovranek; *Modelling heat transfer in heterogeneous media using fractional calculus*; ASME 2011 International Design Engineering Conferences & Computer and Information in Engineering Conference (2011), DETC2011-47374.

[36] A. Dzielinski, D. Sierociuk, and G. Sarwas; *Some applications of fractional order calculus*; Bulletin of the Polish Academy of Sciences - Technical Sciences 58(4)2010.

[37] A. B. Alkhasov, R. P. Meilanov, and M. R. Shabanova; *Heat conduction and heat transfer in technological process: Heat conduction equation in fractional-order derivatives*; Journal of Engineering Physics and Thermophysics 84(2) (March 2011).

[38] V.V. Kulish, and J.L. Lage; *Fractional-diffusion solutions for transient local temperature and heat flux*; Journal of Heat Transfer (May 2001) 372-375.

[39] R. S. Damor, S. Kumar, and A.K. Shukla; *Numerical solutions of fractional bioheat equation with constant and sinusoidal heat flux condition on skin tissue*; American Journal of Mathematical Analysis 1(2013) 20-24.

[40] A. M. Yang, C. Cattani, H. Jafari, and X.J. Yang; *Analytical solutions of the one-dimensional heat equations arising in fractal transient conduction with local fractional derivative*; Abstract and Applied Analysis (2013), Article ID 462535.

[41] J. H. Lienhard; *A heat transfer textbook*, third edition 2013, Massachusetts U.S.A (June 2013).

[42] L. Wang, B. Hu and B. Li; *Validity of Fourier's Law in one-dimensional momentum-conserving lattices with asymmetric interparticle interactions*; Physical Review E 88 052112(2013).

[43] R.H. Yeh and S.P. Liaw; *An exact solution for thermal characteristics of fins with power-law heat transfer coefficient*; International Communications in Heat and Mass Transfer 17 (1990) 317-330.

[44] F. Khani, M. A. Raji, and H. H. Nejad; *Analytic solutions and efficiency of the nonlinear fin problem with temperature-dependent thermal conductivity and heat transfer coefficient*; Communications in Nonlinear Science and Numerical Simulation 14 (2009) 3327-3338.

[45] F. Khani, M. A. Raji and H. Hamedi-Nezhad; *A series solution of the fin problem with a temperature-dependent conductivity*; Communications in Nonlinear Science and Numerical Simulation; 14(7) (2009) 3007-3017.

[46] R. J. Moitsheki, T. Hayat, M.Y. Malik; *Some exact solutions of the fin problem with a power law temperature-dependent thermal conductivity*; Nonlinear Analysis: Real World Applications 11 (2010) 3287-3294.

[47] R.J. Leveque; *A study on numerical methods for hyperbolic conservation laws with stiff source terms*; Journal of Computational Physics 68(1990)187-210.

[48] L. Gosse, G. Toscani; *Asymptotic preserving and well-balanced schemes for radiative transfer and the Rosseland approximation*; Numerische Mathematik 98(2004)223-250.

[49] L. Gosse, G. Toscani; *Space localization and well-balanced schemes for discrete kinetic models in diffusive regimes*; SIAM Journal on Numerical Analysis 41(2004)641-658.

[50] L. Gosse, G. Toscani; *An asymptotic-preserving well-balanced scheme for the hyperbolic heat equations*; Comptes Rendus de l'Acadmie des Sciences - Series I - Mathematics 334(2002)337-342.

[51] I. Rusagara and C. Harley; *Numerical relaxation scheme and mean action time for heat transfer in one dimensional fins of exponential profiles*; Applied Mathematics and Computation 238 (2014) 319328.

[52] A.I. Delis, Th. Katsaounis; *Numerical solution of two-dimensional shallow water equations by application of relaxation methods*; Applied Mathematical Modelling 29 (2005) 754-783.

[53] A.I. Delis, Th. Katsaounis; *Relaxation scheme for shallow water equations*; International Journal for Numerical Methods in Fluids 41 (2003) 695-719.

[54] A. Chalabi; *Convergence of relaxation schemes for hyperbolic conservation laws with stiff source terms*; Mathematics of Computation 68 (1999) 955-970

[55] A. Chalabi and D. Seghir; *Convergence of relaxation schemes for initial boundary value problems for conservation laws*; International Journal - Computers and Mathematics with Applications 43 (2002) 1079-1093.

[56] R. J. LeVeque; *Numerical methods for conservation laws*; Birkhauser Verlag: Basel. Boston. Berlin 1992.

[57] F. Cavalli, G. Naldi, G. Puppo and M. Semplice; *High-order relaxation schemes for non-linear degenerate diffusion problems*; SIAM Journal on Numerical Analysis 45 (2007) 2098-2119.

[58] S. Kim, C.H. Huang; *A series solution of the non-linear fin problem with temperature-dependent thermal conductivity and heat transfer coefficient*; Journal of Physics D: Applied Physics 40 (2007) 2979-2987.

[59] C. Harley; *Asymptotic and dynamical analyses of heat transfer through a rectangular longitudinal fin*; IMA Journal of Applied Mathematics (2013), Article ID 987327.

[60] E. Tadmar; *A review of numerical methods for non-linear partial differential equations*; Bulletin of the American Mathematical Society 49 (October 2012) 507-554.

[61] M. Beck, G. Marchesi, D. Pixton, and L. Sabalka; *A first course in complex analysis*; Binghamton University (SUNY) and San Francisco State University (2012).

[62] I. Rusagara and C. Harley; *Well-balancing and relaxation schemes for the numerical investigation of heat transfer in one dimensional triangular fins*, AIP Conference Proceedings, 1558 (2013) 200-203 .

[63] A. Atangana and I. Rusagara; *On the agaciro equation via the scope of green function*; Mathematical Problems in Engineering (2014), Article ID 201796.

[64] A. Atangana and A. Secer; *A note on fractional order derivatives and table of fractional derivatives of some special functions*; Abstract and Applied Analysis (2013), Article ID 279681.

[65] K. B. Oldham and J. Spanier; *The fractional calculus* , Academic Press, New York, NY, USA, 1974.

[66] I. Podlubny, *Fractional differential equations*, Academic Press, New York, NY, USA, 1999.

[67] A. A. Kilbas, H. M. Srivastava, and J. J. Trujillo; *Theory and applications of fractional differential equations*; Elsevier, Amsterdam, The Netherlands, 2006.

[68] A. Atangana and A. Secer; *Time-fractional coupled-the Korteweg-de Vries equations*; Abstract Applied Analysis (2013), Article ID 947986.

[69] R. W. Ibrahim and H. A. Jalab; *Time-space fractional heat equation in the unit disk*; Abstract and Applied Analysis (2013), Article ID 364042.

[70] F. Yin, J. Song, and X. Cao; *A general iteration formula of VIM for fractional heat- and wave-like equations*; Journal of Applied Mathematics (2013), Article ID 428079.

[71] I. Karatay and S. R. Bayramoglu; *A characteristic difference scheme for time-fractional heat equations based on the Crank-Nicholson difference schemes*; Abstract and Applied Analysis (2012), Article ID 548292.

[72] Y. Z. Povstenko; *Axisymmetric solutions to time-fractional heat conduction equation in a half-space under Robin boundary conditions* ; International Journal of Differential Equations (2012), Article ID 154085.